

**RAMS**  
Reliability, Availability,  
Maintainability, and Safety

# Maintenance Models for Real Time Optimization of Wind Farm Maintenance

Jie Liu

June 2020

MASTER THESIS

Department of Mechanical and Industrial Engineering  
Norwegian University of Science and Technology

Supervisor: Jørn Vatn

## **Abstract**

The thesis intends to study maintenance models for real time optimization of wind turbine maintenance. And then the result could be used to improve the availability of wind farm projects. The experiments of bearing degradation were run in RAMS lab for obtaining real degradation for models testing. It provides a good opportunity to understand the degradation mechanism and chance to practice maintenance models with real data. Some advices are given for improving the experiments in future. Features are extracted from the observations of experiment and selected by the value of monotonicity. Three methods for Cumulative Distribution Function of the first passage time are investigated and implemented. The first passage time is the first time that a stochastic process reaches a certain level. The selected stochastic process are wiener process and Geometric Brownian motion. The results are calculated through designed models with assumed parameters. All results are compared and discussed to give advice on future applications. The first passage time model is compared with digital twin model with the experiment data. The final results are consistent with each other. The benefit of digital twin is self correction during the predict process especially in the later stage. All these models could be used to improve maintenance strategy later.

**Keywords:** Maintenance, Digital Twin, The first passage time, Remaining useful time, Numerical integration, Experiment.

## Preface

The master thesis is continuously working on Digital Twins model for maintenance of Wind Turbines. Some basic work has been done through the Specialization project in autumn semester of 2019. As RAMS engineer, we always attempt to find a better way to improve the system design and operation condition. From the result of Specialization project, Digital Twin could help to improve the maintenance strategies. But there are still problems to be solved before using on real projects. Therefore, models for the first passage time are introduced in spring semester 2020. There are three methods discussed in the thesis to find out the first passage time with Wiener Process and Geometric Brownian Motion. To implement models with real data, an bearing degradation experiment is designed and implemented in RAMS lab. Then data of experiment is used in all these different models and results are compared accordingly. The research is carried out to find out how maintenance models could be used to predict the remaining useful lifetime of bearings and compared with digital twin model.

The thesis is written for master students from RAMS program who has similar interest on the research of maintenance with real time optimization and Digital Twins.

Trondheim, 2020-07-26

(Your signature)

Jie Liu

## Acknowledgment

I would like to thank the valuable help and supervision provided by Jørn Vatn. I do appreciate his patience, encouragement, and professional instructions during the report writing. He gave me great help by providing advice of great value and inspiration of new ideas. When I had problem for the model understanding, he always explained me with patience and clearly plots. Without his consistent support, this report could not been the present form.

Furthermore, I deeply appreciate the help from PhD student Bahareh Tajiani and Mr. Viggo Gabriel Borg Pedersen from RAMS group. They worked on the experiment from the beginning, and support me a lot when I joined the lab. They shared not only the experiment data and settings but also method of research and analysis results. I learned a lot through discussion with them.

Finally, I wish to thank the contribution to this report in various ways by my friends , classmates and families.

Jie Liu

(Your initials)

### Remark:

Given the opportunity here, the RAMS group would recognize Professor Emeritus Marvin Rausand for the work to prepare this template. Some modifications have been proposed by Professor Mary Ann Lundteigen and Professor Jørn Vatn. In the preparation of this revised version important material from Researcher Anita Romsdal has also been included.

## **Executive Summary**

The thesis intends to study maintenance models for real time optimization of wind turbine maintenance. And then the result could be used to improve the availability of wind farm projects. The following work has been done within the thesis:

Firstly, the experiments of bearing degradation are run in RAMS lab for obtaining real degradation for models testing. Although there is still some problems about the experiment setting and data uncertainty, it provides a good opportunity to understand the degradation mechanism and chance to practise maintenance models with real data. Some advice are given for improving the experiments in future.

Secondly, Features are extracted from the observations of experiment and selected by the value of monotonicity.

Thirdly, three methods for Cumulative Distribution Function of the first passage time are investigated and implemented. The first passage time is the first time that a stochastic process reaches a certain level. The selected stochastic process are wiener process and Geometric Brownian motion. The results are calculated through designed models with assumed parameters. All results are compared and discussed to give advice on future applications.

Fourthly, the first passage time model is compared with digital twin model with the experiment data. The final results are consistent with each other. The benefit of digital twin is self correction during the predict process especially in the later stage. All these models could be used to improve maintenance strategy later.

# Contents

Abstract . . . . .	i
Preface . . . . .	ii
Acknowledgment . . . . .	iii
Executive Summary . . . . .	iv
<b>1 Introduction</b>	<b>2</b>
1.1 Background . . . . .	2
1.2 Objectives . . . . .	5
1.3 Approach . . . . .	5
1.4 Contributions . . . . .	6
1.5 Limitations . . . . .	6
1.6 Outline . . . . .	7
<b>2 Theoretical Background</b>	<b>9</b>
2.1 Stochastic Differential Equations . . . . .	9
2.1.1 Wiener Process . . . . .	9
2.1.2 Geometric Brownian Motion (GBM) . . . . .	10
2.2 Experiment Design Theory . . . . .	11
2.2.1 Factorial design of experiments . . . . .	12
2.2.2 Accelerated Life Tests . . . . .	12
2.2.3 Inverse Power Law Model . . . . .	14
2.2.4 Maximum Likelihood Estimation Method . . . . .	14
2.2.5 Principal Component Analysis . . . . .	16
2.3 The First Passage Time . . . . .	17
2.3.1 Inverse Gaussian distribution . . . . .	18
2.3.2 Numerical Integration . . . . .	19
2.3.3 Monte Carlo Simulation . . . . .	21
2.4 Digital Twin . . . . .	21

<b>3</b>	<b>Experiment Design</b>	<b>24</b>
3.1	Experimental Setup . . . . .	24
3.1.1	Preparation of Experiment . . . . .	24
3.1.2	Test Rig . . . . .	25
3.1.3	Bearings . . . . .	25
3.1.4	Accelerometer . . . . .	26
3.1.5	Amplifier . . . . .	27
3.1.6	Software . . . . .	28
3.1.7	Considered factors . . . . .	29
3.2	Experiment Procedure . . . . .	30
3.2.1	Overview . . . . .	30
3.2.2	Procedure . . . . .	30
3.2.3	Data Storage and Feature Extraction . . . . .	31
<b>4</b>	<b>Case Study for the First Passage Time</b>	<b>32</b>
4.1	Wiener Process . . . . .	32
4.1.1	Inverse Gaussian Distribution function . . . . .	32
4.1.2	Numerical integration . . . . .	33
4.1.3	Monte Carlo simulation . . . . .	35
4.1.4	Brief Summary . . . . .	38
4.2	Geometric Brownian motion (GBM) . . . . .	39
4.2.1	Inverse Gaussian Distribution function . . . . .	39
4.2.2	Numerical integration . . . . .	40
4.2.3	Monte Carlo simulation . . . . .	42
4.2.4	Brief Summary . . . . .	46
<b>5</b>	<b>Results</b>	<b>48</b>
5.1	Results of Experiment . . . . .	48
5.1.1	Feature Selection . . . . .	49
5.1.2	Inverse Power Law Model . . . . .	53
5.2	The First Passage Time . . . . .	54
5.2.1	Parameters Estimation through MLE . . . . .	54
5.2.2	Inverse Gaussian Distribution . . . . .	55
5.3	Digital Twin Models . . . . .	57
5.3.1	Feature Extraction and Post-processing . . . . .	57
5.3.2	Feature Importance Ranking and Fusion . . . . .	58
5.3.3	Model Fitting and Prediction . . . . .	60
5.3.4	Performance Analysis . . . . .	62

<i>CONTENTS</i>	1
<b>6 Discussion</b>	<b>64</b>
6.1 Experiment Design . . . . .	64
6.2 Maintenance Models . . . . .	65
6.2.1 The First Passage Time Models . . . . .	65
6.2.2 Digital Twin Model . . . . .	66
6.2.3 Comparison between Models . . . . .	67
<b>7 Conclusions</b>	<b>69</b>
7.1 Conclusions . . . . .	69
7.2 Discussion . . . . .	70
7.3 Recommendations for Further Work . . . . .	70
<b>A Acronyms</b>	<b>72</b>
<b>B Form for Experiment Record</b>	<b>73</b>
<b>C Plot of RUL Result of Digital Twin with Experiment Data</b>	<b>76</b>
<b>References</b>	<b>83</b>



# Chapter 1

## Introduction

### 1.1 Background

Wind Turbines have been designed and used in different countries for many years. It can convert wind energy to electrical energy with less or no pollution and consumption of other resources. With the concern of environment, many countries start to develop large wind turbine farms to generate stable, safe and clean energy. As there are a lot of benefit for offshore wind farms such as higher mean wind speed compared with onshore projects, greater area available for siting large projects, lower turbulence intensities and wind shear ([Manwell et al. \(2010\)](#)), many wind farms are built as offshore projects. But the harsh working conditions caused more failures and limited accessibility for frequently maintenance and lower production. According to the statistics of [Faulstich et al. \(2011\)](#), 75% of all failures are minor failures and are responsible for only 5% of downtime for onshore wind turbine projects. That's why most researches about wind turbines are focused on major failures which caused longer downtime. However, the affect of the minor failures are amplified for offshore projects due to the longer waiting, traveling and repairing time. Therefore, it is necessary to pay more attention to the minor failures such as bearings to enhance the availability of wind turbine projects.

Models are needed to study the degradation of wind turbine components. While for many components such as bearings, it is not straight forward to use readings from condition monitoring directly. Features shall be extracted from the monitoring results and used in the degradation models. [Saidi et al. \(2017\)](#) and [Ali et al. \(2018\)](#) gives some typical statistics features for time-domain signal. Then the models could be used to predict the remaining useful life or the first passage time of the degradation. Remaining useful life (RUL) is the length of time a component is likely to operate before it requires repair or replacement. It is a stochastic variable and estimate according to the information of system and component status. Examples are given by [Phuc et al. \(2012\)](#) and [Qin et al. \(2017\)](#). The first passage time is also called the first hitting time

or the first exit time. It is the first time that a stochastic process reaches a certain level which is called threshold. There are many articles working on this topic and give demonstration on how to find out the first passage time under different assumption. Examples are given by [Urdapilleta \(2011\)](#) and [Galván-Núñez & Attoh-Okine \(2018\)](#). While there are many models working on different stochastic process and it is hard to make choice which model shall be used for prediction.

To test the degradation models, data from experiments or real life operations are needed. But there is few experiment data about degradation published. And the public experiment data is either lack the necessary information about the experiment settings or just single set of data which is hard to verify. To better implement degradation models, it is necessary to have data which is fully understood about the setting of data and mechanisms of experiments.

With the development of Computer Science, it is possible to use digital twin model to deal with data and operational conditions in "real time" and use the degradation models and RUL prediction to optimize maintenance. Digital Twin is one of the technology for modeling. The definition was firstly introduced by Dr. Michael [Grieves \(2014\)](#) in 2002. A digital twin is a digital replica of a living or non-living physical entity defined by [Saddik \(2018\)](#). More and more companies start to look at the method and try to find out if it could be implemented in their own business. According to the preliminary literature review, there are few results about the digital twin models used on maintenance optimization. It means that it is hard to find a good example or a built-up model for the research, but also means that there are not many jobs done for this particular topic.

## **Problem Formulation**

Literature review has been carried out during the specialization project in fall semester of 2019. There are still many gaps between the industry requirement and current research achievements. To improve the availability of offshore wind farms, the suitable maintenance models shall be selected for minor failures prediction which could help owners to do predictive maintenance for cost saving and enhancing productivity of projects. While there are so many models, and wrong model might lead to wrong decisions. Therefore, the comparison between those models are necessary. To improve the maintenance, digital twin model shall be considered and compared as well. For testing those models, real degradation data is needed to find out which model is better for the predictions. How to extract feature and use selected features for prediction is also a problem to be solved, especially for those components cannot use observed information directly for prediction such as bearings.

## Related work

The following books and articles are used for studying as the start of the project.

- Reliability of Safety-Critical Systems: Theory and Applications. [Rausand \(2014\)](#). The book provide a comprehensive introduction to reliability assessments of safety related system. The book presents theory and methods used to improve the operations and maintenance of critical system.
- System Reliability Theory: Models, Statistical Methods, and Applications. [Rausand & Høyland \(2004\)](#). The book is a fundamental textbook for reliability theory. It gives a comprehensive introduction for reliability analysis. In addition, it introduced many analytical tools such as Markov processes, life data analysis, accelerated life testing, features numerous worked examples.
- Wind energy explained: theory, design and application [Manwell et al. \(2010\)](#). It is the textbook of PhD course BA8607 - Design of offshore wind turbines. The book gives overall introduction to offshore wind energy, with a focus on the design of wind turbines. The book helps to consider maintenance from the design perspective.
- PK8207 - Lecture memo for Numerical integration of stochastic processes. [Vatn \(2020\)](#). It is the learning material of PhD course PK8207 - Maintenance Optimisation. The course introduced several maintenance models for stochastic processes with numerical integration methods.

## What Remains to be Done?

As discussed above, there are still some problems be solved. The research will try to answer below questions:

- Where can get real degradation data for bearings degradation?
- How to obtain and select features from the observed data?
- How to use selected features to predict RUL of components?
- How to use selected features to find out the first passage time of stochastic degradation?
- Is the digital twin model can help to improve current maintenance models?

## 1.2 Objectives

The project goal is trying to find better maintenance strategy for maintenance of wind farm. Digital Twin model is compared with maintenance models for models improvement. The main objectives of this Master's project are

1. Investigate design of RAMS experiment of bearings degradation.
2. Conduct designed experiments and obtain real degradation data.
3. Investigate the features obtain and selection methods from experiment data.
4. Investigate the maintenance models for the first passage time model with stochastic process. The suggested stochastic process are wiener process and Geometric Brownian motion.
5. Implement maintenance models and digital twin model with data from experiments.
6. Compare the maintenance models with digital twin model.

## 1.3 Approach

Here lists the approach that are used to meet the objectives and tasks.

1. Join the PhD project of RAMS lab about bearing degradation and run experiment under instruction of PhD students.
2. Literature review for experiment design.
3. Find out requirements, equipment and methods for experiment running.
4. Literature review for statistics methods of data processing.
5. Literature review for terminology of maintenance models.
6. Literature review for the terminology of stochastic process, wiener process and Geometric Brownian motion.
7. Literature review for maintenance model of the first passage time.
8. Create models for the first passage time.
9. Compare the methods for calculating the first passage time models with assumed parameters. Choose one method as maintenance model.

10. Use experiment data on maintenance model and digital twin model.
11. Compare results of models for better maintenance strategy.

## 1.4 Contributions

Here is a list of main contributions in the project work.

- Literature review for Wiener process, Geometric Brownian motion, the first passage time, experiment design, statistic methods such as maximum likelihood estimation and principal component analysis.
- Implement and compare three methods for the first passage time models with wiener process and GBM respectively.
- Complete experiment design for bearing degradation.
- Implement experiment.
- Extract and select features from experiment results.
- Analyse experiment data with the first passage time model and digital twin model.
- Comparison of results from two models.

## 1.5 Limitations

The scope of the thesis will be limited by time, COVID-19 and tools.

- **Time constraint**

The thesis is limited by the time constraints since the deadline for submission is July, 2020. The work includes experiment of bearings which may cost more time due to implement of experiment.

- **Corona-virus Situation**

Due to the COVID-19, campus has to be closed in March. There is no access for physical library and other resources such as printing. In addition, the experiment is postponed due to close of RAMS lab.

- **Limited tools for the study**

The study might be limited by tools used for research, such as computer capacity, access of software and additional equipment for experiment.

## 1.6 Outline

Below is an overview of how the remaining part of the report is organized:

- **Preface.**

Contains practical information about what has been done, and where the work has been carried out and any assumed background of the reader.

- **Acknowledgments.**

The gratitude to who have been supporting to the work, professionally and family as relevant.

- **Summary.**

It summarizes what has been done for the thesis and explained why it is important.

- **Chapter 1. Introduction of the project.**

It introduced the background, objective, approach and outline of the thesis.

- **Chapter 2. Theoretical background.**

The section presents the terminology and methods used in the thesis. Literature review is carried out for experiment design, statistic methods for data processing, wiener process, Geometric Brownian motion, the first passage time and digital twins. Functions used for models are listed and approved. The review of resources provides the necessary theoretical foundation for the implementation of experiment design, data processing and models development.

- **Chapter 3. Experiment Design.**

The experiment is designed according to the theories introduced in chapter 2.

- **Chapter 4. Case study for the first passage time models.**

The first passage time models are implemented with assumed parameters. This is to verify the methods and to prepare for data analysing of real data.

- **Chapter 5. Results.**

The results from experiment are present. Features are extracted and inputted in the first passage time model and digital twin model.

- **Chapter 6. Discussion.**

Results from previous chapter are discussed and analysed.

- **Chapter 7. Conclusions and ideas for further work.**
- **Appendix A. Acronyms**
- **Appendix B. Form for experiment record**
- **Appendix C. Plot of RUL Result of digital twin**
- **Bibliography**

# Chapter 2

## Theoretical Background

In this section, the theoretical background for experiment design and selected maintenance models were given and discussed. It is an overview of the research and literature present in the field and shows the state-of-the-art within RAMS experiment and maintenance models used for wind turbines. Limitations for maintenance models are discussed. The tools for literature review are **Oria** and **Google Scholar**. Searching Key Words are the combinations of **Maintenance**, **Experiment**, **RAMS**, **Wiener Process (Brownian Motion)**, **Geometric Brownian Motion**, **First Passage Time** and **Digital Twin**. The result is discussed with following sections.

### 2.1 Stochastic Differential Equations

#### 2.1.1 Wiener Process

The Wiener process is a real valued continuous-time stochastic process named in honor of American mathematician Norbert Wiener for his investigations on the mathematical properties of the one-dimensional Brownian motion [Wiener \(1976\)](#). It is widely used in mathematics, applied mathematics, economic [Tseng et al. \(2003\)](#), finance [Cheridito \(2001\)](#), physics [Blasi et al. \(1997\)](#), biology [Dennis et al. \(1991\)](#) and so on. In addition, it is a very popular model method for reliability evaluation of high reliable products [Ye & Xie \(2015\)](#). As shown in the searching result of "Wiener Process", there are more than one thousand books or articles using wiener process as their subject. If the searching key words "Maintenance" or "RUL" is added, the number of articles dropped to less one hundred.

The definition of wiener process can be characterized as

- $W(0) = 0$ ;



- $W(t)$  is continuous;
- $W(t)$  has independent increments;
- $W(t) - W(s) \sim \mathbb{N}(0, t - s)$ , for  $0 \leq s \leq t$ .

where  $\mathbb{N}(\mu, \sigma^2)$  presents the normal distribution with expected value  $\mu$  and variance  $\sigma^2$ .

Then the degradation process can be defined as Equation 2.1

$$Y(t) = y_0 + \mu t + \sigma W(t) \quad (2.1)$$

where  $y_0$  represents the initial degradation level,  $\mu$  is drift coefficient and  $\sigma$  is diffusion coefficient,  $W(t)$  is a normalized Wiener process. With above equation, for each increment of degradation, we have Equation 2.2

$$\Delta Y = Y(t) - Y(s) \sim \mathbb{N}(\mu(t - s), \sigma^2(t - s)), 0 \leq s \leq t \quad (2.2)$$

where  $\Delta Y$  follows normal distribution with expected value  $\mu(t - s)$  and variance  $\sigma^2(t - s)$ . Since  $\mu$  and  $\sigma$  do not change for each degradation, the distribution is constant if the time interval are same. This means the increments only depend on time and are not related to the previous degradation levels. It is not matching some failure mechanism such as the fatigue cracks equation described by Paris' law (Paris & Erdogan (1963)). Therefore, Geometric Brownian Motion is introduced since the increments depend on both current degradation level and time intervals.

### 2.1.2 Geometric Brownian Motion (GBM)

Geometric Brownian motion is to describe a stochastic process which satisfies the following equation:

$$dS(t) = \mu S(t) dt + \sigma S(t) dW(t) \quad (2.3)$$

where  $W(t)$  is a normalized Wiener process and the notation  $d$  is denoting the increment in a small time interval of length  $dt$ .  $\mu$  is "the percentage drift" and  $\sigma$  is "the percentage volatility". Then for each increment  $dS(t)$ , it follows normal distribution with mean value  $\mu S(t) dt$  and variance  $\sigma^2 S(t)^2 dt$ . Therefore, it has be calculated step by step.

To build the relationship to the initial state directly, another definition for GBM is introduced. GBM is also called as exponential Brownian motion Ross (2014). Let  $f(S) = \log S_t$ , then

according to *Itô's lemma* we have below equations [Itô \(1944\)](#)

$$\begin{aligned}
 d\log(S_t) &= f'(S_t)dS_t + \frac{1}{2}f''(S_t)S_t^2\sigma^2 dt \\
 &= \frac{1}{S_t}(\sigma S_t dW(t) + \mu S_t dt) - \frac{1}{2}\sigma^2 dt \\
 &= \left(\mu - \frac{\sigma^2}{2}\right)dt + \sigma dW(t)
 \end{aligned} \tag{2.4}$$

Then we have

$$\log(S_t) = \log(S_0) + \left(\mu - \frac{\sigma^2}{2}\right)t + \sigma W(t) \tag{2.5}$$

Exponentiate both sides of above equation, expression for  $S_t$  is as below.

$$\begin{aligned}
 S(t) &= e^{\log(S_0) + \left(\mu - \frac{\sigma^2}{2}\right)t + \sigma W(t)} \\
 &= S_0 \exp\left(\left(\mu - \frac{\sigma^2}{2}\right)t + \sigma W(t)\right)
 \end{aligned} \tag{2.6}$$

where  $S_0$  is the initial state. It is clear that if the initial value  $S_0 = 0$ , then the whole process will be equal to 0 which means there is no development of process. This corresponds to a situation where a perfect piece of material will not have fatigue cracks. In order to use the GBM, the initial state shall be assumed to be positive. Furthermore, GBM follows log-normally distribution. The mean value is  $\log S_0 + \left(\mu - \frac{\sigma^2}{2}\right) * t$  and variance is  $\sigma^2 t$ . If  $\mu - \frac{\sigma^2}{2} \leq 0$ , the process might go backwards and being absorbed at zero. Therefore, the drift parameter  $\mu$  shall always be larger than  $\frac{\sigma^2}{2}$ . Finally, it is obvious that the increment depends on time interval and the current location in the progress which is appropriate to model degradation.

## 2.2 Experiment Design Theory

Experimental design is the design of any task that aims to describe and explain the variation of information under conditions that are hypothesized to reflect the variation. It is an integral component of quality improvement, and supports improvement in product design, process design and process operation. Therefore, the following items need to be clarified before the start of experiment. [Fisher \(1936\)](#)

- Purpose of experiment
- Responses of experiment
- Factors which can be manipulated

- Operating region and times
- Testing budget

### 2.2.1 Factorial design of experiments

Before experiment, the responses of experiment shall be investigated. Relationship between responses and factors shall be estimated firstly. There are some methods to estimate the importance of factors and interaction between factors, such as Main Effect ([Montgomery \(2017\)](#)), ANOVA ([Fisher \(1992\)](#)) and so on. Then the experiment can decide which factors are included and how factors are varied. If there are  $k$  factors under investigation, a  $n$ -level factorial design will consist of  $n^k$  runs at least ([Fisher \(1936\)](#)). The precise of result can be obtained by increasing the number of testing. The experiment shall be upgraded according to the result of testing to get more precise parameters of function.

### 2.2.2 Accelerated Life Tests

According to [Manwell et al. \(2010\)](#), the average availability of wind turbines is around 99%. This means the devices used in Wind Turbines are highly reliable under the normal operation conditions. To have an experiment result within a reasonable time, accelerated life testing (ALT) is a common way to be implemented. The approach is to expose the devices to an overstress condition in order to cut down MTTF (Mean Time to Failure) to an acceptable level [Nelson \(1980\)](#). Depending on the type of devices, the stress may involve a high level of temperature, pressure, load, frequency and so on. There may be only one stress with different levels or several stress working on the devices. The stress can increase step by step which is called SALT (Step-stress accelerated tests). In the other hand the stress can increase continuously which is called PALT (Progressive-stress Accelerated Tests). [Rausand & Høyland \(2004\)](#)

For the simplest situation, there shall be only one stress increased during the process. There are two basic methods to design this kind of experiment. The first one is to run experiment on one stress level until failure and repeat the process on different stress levels. The number of experiment shall be large to make the results independently. The second method is to run experiment on different stress levels with different time period until the unit is failed. This methods is more efficient and cost saving compared with the first method. It is suitable when the samples number is limited.

If there is more than one stress, it is similar with the second method mentioned above. Different stress can be treated as different level of single stress. While to simplify the analysis, it

shall avoid to add more than one level or stress at the same time.

Rausand & Høyland (2004) proposed a method to get the parameters of SALT experiments under two stress levels which is explained as below. The process is shown as Figure 2.1.

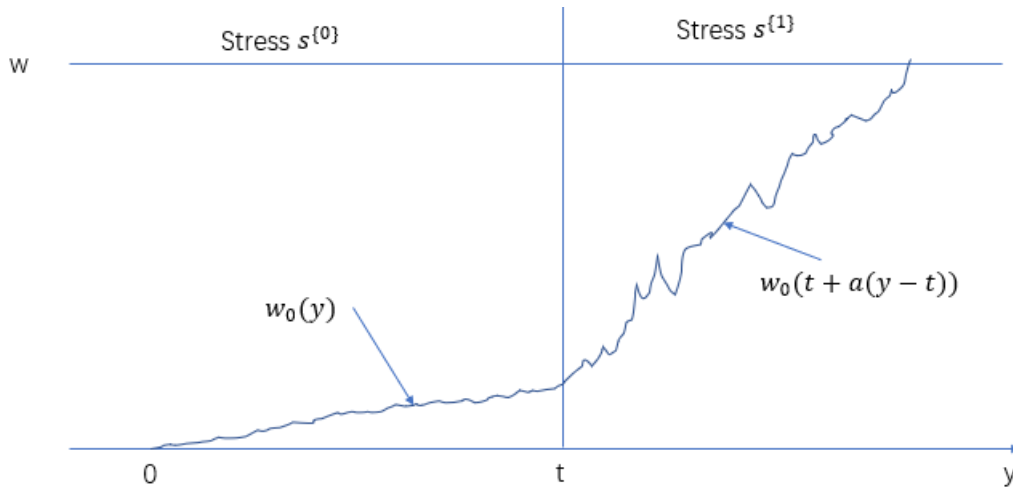


Figure 2.1: Fatigue process  $W(y)$  with stress level increased from  $s^{(0)}$  to  $s^{(1)}$  at time  $t$

- The stress level is raised up during the process,
- For the first time interval  $(0, t_0]$ , the stress level is  $s^{(0)}$ . For the second time interval  $(t_0, t_1)$ , the stress level is  $s^{(1)}$  and so on.
- Assume the degradation of bearing follows Brownian motion, therefore, Wiener process model can be used for data analyzing.
- $\{W_0(y), y \geq 0\}$ , with drift  $\mu > 0$  and diffusion constant  $\sigma^2 > 0$ .
- $W_0(y_2 - y_1) \sim \mathcal{N}(\mu(t_2 - t_1), \sigma^2(t_2 - t_1))$ , for  $0 < y_1 < y_2$
- $W_1(y) = W_0(t + \alpha(y - t))$ , for  $y > t$ ,  $\alpha > 1$
- Then the parameters can be obtained by Maximum Likelihood Estimation Method which is introduced later.
- The method requires long time operation under one stress level which doesn't implemented in the experiment. The reason is the data has to be saved manually, and lab is not allowed to use after working time due to the building control.

### 2.2.3 Inverse Power Law Model

The Inverse Power Law Model is commonly used when the life of system is an inverse power function of a non-thermal acceleration stress (Nelson (1972)). The definition is given as Function 2.7.

$$L(V) = \frac{1}{KV^n} \quad (2.7)$$

where L is a quantifiable life measure, V is the stress level, K and n are positive parameters which characteristic of the device and the test method.

Then for any two stresses,  $V_1$  and  $V_2$ , we can get Equation 2.8

$$\frac{L_2}{L_1} = \left(\frac{V_1}{V_2}\right)^n \quad (2.8)$$

The method can be used to estimate the life measure with different stress level and verify the result of different experiment.

### 2.2.4 Maximum Likelihood Estimation Method

In statistics, maximum likelihood estimation (MLE) is a method of estimating the parameters of a probability distribution by maximizing a likelihood function, so that under the assumed statistical model the observed data is most probable. The point in the parameter space that maximizes the likelihood function is called the maximum likelihood estimate Rossi (2018). It is a dominant means of statistical inference, examples can be referred to Hendry & Nielsen (2007), Chambers et al. (2012) etc.

To use MLE method, statistical model shall be selected first. Here wiener process and GBM are selected for discussion respectively. The formulas derivation referred to Hu et al. (2018) with necessary modified.

#### Wiener Process

Assume we obtained data as following:  $(t_0, Y_0), (t_1, Y_1), (t_2, Y_2), \dots, (t_n, Y_n)$ , where  $t_i$  is time and  $Y_i$  is degradation level of health indicator. Then the increment of health indicator which follows wiener process is given as Equation 2.9

$$\Delta Y_i = \mu \Delta t_i + \sigma \Delta W(t_i) \quad (2.9)$$

where  $\Delta Y_i = Y_i - Y_{i-1}$ ,  $\mu \Delta t_i = \mu(t_i - t_{i-1})$ , and  $\sigma \Delta W(t_i) = \sigma[W(t_i) - W(t_{i-1})]$ , ( $i = 1, 2, \dots, n$ ). According to Equation 2.2,  $\Delta Y$  follows normal distribution which can be rewritten as Equation 2.10

$$\Delta Y_i \sim \mathbb{N}(\mu \Delta t_i, \sigma^2 \Delta t_i) \quad (2.10)$$

The sample likelihood function  $L(\mu, \sigma)$  can be obtained by Equation 2.11 based on the wiener process.

$$\begin{aligned} L(\mu, \sigma) &= f(\Delta Y_1, \Delta Y_2, \dots, \Delta Y_n) \\ &= f(\Delta Y_1) f(\Delta Y_2) \dots f(\Delta Y_n) \\ \ln L(\mu, \sigma) &= \ln f(\Delta Y_1) + \ln f(\Delta Y_2) + \dots + \ln f(\Delta Y_n) \end{aligned} \quad (2.11)$$

For normal distributed  $f(\Delta Y_i)$ , we have:

$$\begin{aligned} f(\Delta Y_i) &= \frac{1}{\sigma \sqrt{\Delta t_i} \sqrt{2\pi}} e^{-\frac{1}{2} \left( \frac{\Delta Y_i - \mu \Delta t_i}{\sigma \sqrt{\Delta t_i}} \right)^2} \\ \ln f(\Delta Y_i) &= \ln \left( \frac{1}{\sigma \sqrt{\Delta t_i} \sqrt{2\pi}} \right) - \frac{1}{2} \left( \frac{\Delta Y_i - \mu \Delta t_i}{\sigma \sqrt{\Delta t_i}} \right)^2 \end{aligned} \quad (2.12)$$

The partial differential equations with respect to  $\mu$  and  $\sigma$  are given in Equations 2.13 and 2.14.

$$\frac{\partial \ln L}{\partial \mu} = \sum_{i=1}^n \left( \frac{\Delta Y_i - \mu \Delta t_i}{\sigma^2} \right) = 0 \quad (2.13)$$

$$\frac{\partial \ln L}{\partial \sigma} = \sum_{i=1}^n \left( -\frac{1}{\sigma} + \frac{(\Delta Y_i - \mu \Delta t_i)^2}{\Delta t_i \sigma^3} \right) = 0 \quad (2.14)$$

According to above Equations, the maximum likelihood estimate  $\hat{\mu}$  and  $\hat{\sigma}$  can be calculated as following.

$$\hat{\mu} = \frac{1}{n} \sum_{i=1}^n \frac{\Delta Y_i}{\Delta t_i} \quad (2.15)$$

$$\hat{\sigma} = \left[ \frac{1}{n} \sum_{i=1}^n \frac{(\Delta Y_i - \hat{\mu} \Delta t_i)^2}{\Delta t_i} \right]^{\frac{1}{2}} \quad (2.16)$$

### Geometric Brownian Motion

The process to get parameters for SDE of GBM is almost same with wiener process. According to Equation 2.3,  $\Delta S(t_i)$  follows normal distribution which can be present as Equation 2.17

$$\Delta S(t_i) \sim \mathbb{N}(\mu S(t_i) \Delta t_i, \sigma^2 S^2(t_i) \Delta t_i) \quad (2.17)$$

where  $\Delta S(t_i) = S(t_i) - S(t_{i-1})$ . For PDF of  $f(\Delta S(t_i))$ , we have

$$f(\Delta S(t_i)) = \frac{1}{\sigma S(t_i) \sqrt{\Delta t_i} \sqrt{2\pi}} e^{-\frac{1}{2} \left( \frac{\Delta S(t_i) - \mu S(t_i) \Delta t_i}{\sigma S(t_i) \sqrt{\Delta t_i}} \right)^2} \quad (2.18)$$

$$\ln f(\Delta S(t_i)) = \ln \left( \frac{1}{\sigma S(t_i) \sqrt{\Delta t_i} \sqrt{2\pi}} \right) - \frac{1}{2} \left( \frac{\Delta S(t_i) - \mu S(t_i) \Delta t_i}{\sigma S(t_i) \sqrt{\Delta t_i}} \right)^2$$

Then we use Equation 2.11 and 2.18 and to get partial differential equations with respect to  $\mu$  and  $\sigma$ . The equations are given as Equation 2.19 and 2.20.

$$\frac{\partial \ln L}{\partial \mu} = \sum_{i=1}^n \left( \frac{\Delta S(t_i) - \mu S(t_i) \Delta t_i}{\sigma^2 S(t_i)} \right) = 0 \quad (2.19)$$

$$\frac{\partial \ln L}{\partial \sigma} = \sum_{i=1}^n \left( -\frac{1}{\sigma} + \frac{(\Delta S(t_i) - \mu S(t_i) \Delta t_i)^2}{S^2(t_i) \Delta t_i \sigma^3} \right) = 0 \quad (2.20)$$

Therefore, the maximum likelihood estimate  $\hat{\mu}$  and  $\hat{\sigma}$  can be calculated as following Equation 2.21 and 2.22.

$$\hat{\mu} = \frac{1}{n} \sum_{i=1}^n \frac{\Delta S(t_i)}{S(t_i) \Delta t_i} \quad (2.21)$$

$$\hat{\sigma} = \left[ \frac{1}{n} \sum_{i=1}^n \frac{(\Delta S(t_i) - \hat{\mu} S(t_i) \Delta t_i)^2}{S^2(t_i) \Delta t_i} \right]^{\frac{1}{2}} \quad (2.22)$$

Note: The accuracy of MLE depends on the number of samples. When the number of samples drops from 1000 to 100, the difference between the estimated parameters increased from 5% to 15% (estimated by Monte Carlo simulation).

### 2.2.5 Principal Component Analysis

Principal component analysis is a very popular multivariate statistics method to analysis multiple features. It is firstly present by Pearson (1901) and developed by many researchers after that. The method could transfer the data to a new coordinate system which is orthogonal linear transformation and the greatest variance of data comes to lie on the first principal component, the second greatest variance on the second coordinate, and so on (Jolliffe (1986)). Generally, the number of principal component is same with the features considered. The methods could help to keep most of information from original data with less dimensions. For example, if the first principal component keep most of the information, the others components can be ignore

during further calculation which simplified the analysis process.

The method is also well used in maintenance area. If there are many explanatory variables or features, it is beneficial to reduce the number of variables with the help of PCA. Here are the examples where PCA is used in prognostics, diagnosis and status monitoring, such as reducing sensor complexity for monitoring wind turbine performance by PCA ( [Y. Wang et al. \(2016\)](#)), Indirect health monitoring of bridges using Mel-frequency cepstral coefficients and principal component analysis ( [Mei et al. \(2019\)](#)), A new tool wear monitoring method based on multi-scale PCA ( [G. Wang et al. \(2019\)](#)) and so on.

## 2.3 The First Passage Time

The first passage time is also called the first hitting time or the first exit time. It is the first time that a stochastic process reaches a certain level which is called threshold ([Barros \(2019\)](#)). There are two basic components in a first passage time model. The first is the stochastic process, the second is a boundary set or threshold. The threshold could be a fixed value, or variable above zero ([Caroni \(2017\)](#)). To simplify the calculation, the thesis only considered the threshold as fixed value.

The distribution of the first passage time can help us understand better the property of system failure. Research on this area started one hundred years ago, and it has been discussed in many books with different subjects [Redner \(2001\)](#). Since the process is stochastic, the first passage time is uncertain with different distribution models. Some researchers focus on Mean first-passage time such as [Thomas \(1975\)](#), [Murthy & Kehr \(1989\)](#), [Jing-Yuan et al. \(2012\)](#) since it can provide the first impression of first passage time. While the variance is depended on the distribution of selected models which shall be discussed individually. Wiener process (Eg. [Shepp \(1967\)](#)) and Geometric Brownian Motion (Eg. [Abundo \(2010\)](#)) are often selected as basic distribution.

Within the thesis, three methods are used to calculate the CDF of the first passage time which are Inverse Gaussian distribution, numerical integration and Monte Carlo simulation. These methods will be discussed in the following sections individually.



### 2.3.1 Inverse Gaussian distribution

As explained by [Sato & Inoue \(1994\)](#), the first passage time of Wiener Process follows Inverse Gaussian distribution. The CDF of first passage time is shown as Equation 2.23.

$$F_T(t) = \Phi\left(\frac{\sqrt{\lambda}}{\nu}\sqrt{t} - \sqrt{\lambda}\frac{1}{\sqrt{t}}\right) + \Phi\left(-\frac{\sqrt{\lambda}}{\nu}\sqrt{t} - \sqrt{\lambda}\frac{1}{\sqrt{t}}\right)e^{2\lambda/\nu} \quad (2.23)$$

where  $\nu = L/\mu$  and  $\lambda = L^2/\sigma^2$ . Then the distribution of the first passage time  $\rho$  for Wiener process can be written as

$$\rho \sim IG\left(\frac{L}{\mu}, \frac{L^2}{\sigma^2}\right) \quad (2.24)$$

The Mean Time and Variance of the first passage time can be calculated with Equation 2.25 and 2.26 in terms of the original parameters.

$$E(T) = \nu = \frac{L}{\mu} \quad (2.25)$$

$$Var(T) = \frac{\nu^3}{\lambda} = \frac{L\sigma^2}{\mu^3} \quad (2.26)$$

For Geometric Brownian Motion, [Primožic \(2011\)](#) has approved that it follows the same distribution with the exponential definition shows as Equation 2.6. The CDF of the first passage time is Equation 2.23 too. Where  $\nu = \frac{\log L - \log S_0}{\mu - \frac{1}{2}\sigma^2}$  and  $\lambda = \frac{(\log L - \log S_0)^2}{\sigma^2}$ . The distribution of the first passage time  $\rho$  for GBM can be present as Equation 2.27.

$$\rho \sim IG\left(\frac{\log L - \log S_0}{\mu - \frac{1}{2}\sigma^2}, \frac{(\log L - \log S_0)^2}{\sigma^2}\right) \quad (2.27)$$

The Mean Time and Variance of the first passage time can be calculated with Equation 2.28 and 2.29.

$$E(T) = \nu = \frac{\log L - \log S_0}{\mu - \frac{1}{2}\sigma^2} \quad (2.28)$$

$$Var(T) = \frac{\nu^3}{\lambda} = \frac{\sigma^2(\log L - \log S_0)}{(\mu - \frac{1}{2}\sigma^2)^3} \quad (2.29)$$

These functions can be used to get the CDF of the first passage time directly and results are quite promising since it can be approved.

### 2.3.2 Numerical Integration

Numerical integration is one way to find the first passage CDF. The method is introduced by Professor Jørn Vatn in the PhD course PK8207 (Vatn (2020)).

Let  $y$  be the degradation level. If the PDF of the degradation level at time  $t$  is known, the law of total probability gives the PDF of the deterioration level at time  $t + dt$  as:

$$f(y | t + dt) = \int_{-\infty}^{\infty} f(y - s | t)g(s)ds \quad (2.30)$$

since we have assumed the a failure occurs when the degradation level exceed the threshold  $L$ , the Equation 2.30 can be rewritten as Equation 2.31.

$$f(y | t + dt) = \int_{y-L}^{\infty} f(y - s | t)g(s)ds \quad (2.31)$$

where  $f(y - s | t)$  is the PDF of  $(y - s)$  at time  $t$ ,  $g(s)$  is PDF of increment  $s$ . The equation described the degradation level from  $(y - s)$  to  $y$  by increased  $s$  from time  $t$  to time  $t + dt$ .

If we can integrate Equation 2.31 numerically, the CDF of the first passage time can be obtained at any point of time by Equation 2.32.

$$F_T(t) = Pr(T \leq t) = 1 - \int_{-\infty}^L f(y | t)dy \quad (2.32)$$

From the definition of wiener process (Equation 2.2) and GBM (Equation 2.3), the increments follow normal distribution. Then we use  $g(s | t)$  to present the PDF of the increment from time  $t$  to  $t + dt$ .

To integrate Equation 2.31, we firstly save  $f(y | t)$  in an array which is denoted as  $f$ . Then for any value of  $y_i$ , we can denoted as  $f(i) = f(y_i | t)$ , where  $y_i = idy$  and  $dy = L/n$ .  $dy$  is the interval length and  $n$  is assumed large enough to get the appropriate result.

If we divide  $f(y - s | t)$  to very small interval, it can be treated as linear function. Then the integration is changed to the integration of product of linear function and normal distribution. If we found out the function of  $f(y - s | t)$ , the integration can be obtained from the iteration of Equation 2.33.

$$f(y_i | t + dt) = \sum_j \int_{(j-1)dy}^{jdy} f(y_i - s | t)g(s)ds \quad (2.33)$$

Assume  $f(y) = a'y + b'$ , then we have  $f(y_i - s) = as + b = -a's + (b' + a'y_i)$ . Where  $a = a'$  and

$b = b' + a'y_i$ . The parameter  $-a'$  and  $b'$  can be calculated by the value of  $f(i - j)$  and  $f(i - j + 1)$  which obtained from the previous iteration of Equation 2.31.

Equation 2.33 is turned to

$$\begin{aligned}
 f(y_i | t + dt) &= \sum_j \int_{(j-1)dy}^{jdy} f(y_i - s | t) g(s) ds \\
 &= \sum_j \int_{(j-1)dy}^{jdy} (as + b) g(s) ds \\
 &= \sum_j \left( a * \int_{(j-1)dy}^{jdy} s * g(s) ds + b * \int_{(j-1)dy}^{jdy} g(s) ds \right) \\
 &= \sum_j (a * A + b * B)
 \end{aligned} \tag{2.34}$$

According to **Result 2.3** of [Vatn \(2019\)](#), if  $X$  follows normal distribution with parameter  $\mu$  and  $\sigma$  then :

$$\int_{-\infty}^{\beta} x f(x) = \mu \Phi \left( \frac{\beta - \mu}{\sigma} \right) - \sigma \phi \left( \frac{\beta - \mu}{\sigma} \right) \tag{2.35}$$

where  $\Phi()$  and  $\phi()$  are the CDF and PDF for the standard normal distribution respectively.

Then we have

$$\begin{aligned}
 A &= \int_{(j-1)dy}^{jdy} s * g(s) ds \\
 &= \int_{-\infty}^{jdy} s * g(s) ds - \int_{-\infty}^{(j-1)dy} s * g(s) ds \\
 &= \left[ \mu \Phi \left( \frac{jdy - \mu}{\sigma} \right) - \sigma \phi \left( \frac{jdy - \mu}{\sigma} \right) \right] - \left[ \mu \Phi \left( \frac{(j-1)dy - \mu}{\sigma} \right) - \sigma \phi \left( \frac{(j-1)dy - \mu}{\sigma} \right) \right]
 \end{aligned} \tag{2.36}$$

where  $\mu$  and  $\sigma$  are parameters of  $g(s)$ .

For  $B$ , it can be turned to PDF of the standard normal distribution as well.

$$\begin{aligned}
 B &= \int_{(j-1)dy}^{jdy} g(s) ds \\
 &= \phi \left( \frac{jdy - \mu}{\sigma} \right) - \phi \left( \frac{(j-1)dy - \mu}{\sigma} \right)
 \end{aligned} \tag{2.37}$$

Therefore, we can solve Equation 2.31 if we have the first integration  $f(1)$ . Since we always know the initial state, then  $f(1)$  is PDF of normal distribution  $g(s)$ . The equation are solved accordingly.

**Remark:**

The initial state for wiener process is 0, while it can not be 0 for GBM. In addition, the parameters of the normal distribution for increments are different for wiener process and GBM. Details have been explained in Section [2.1.1](#) and [2.1.2](#).

**2.3.3 Monte Carlo Simulation**

Monte Carlo Simulation is a broad used method which is to repeat random sampling to obtain numerical results. Monte Carlo methods are mainly used in three problem classes: optimization, numerical integration, and generating draws from a probability distribution ([Kroese et al. \(2014\)](#)). Since the numerical approach is difficult, Monte Carlo simulation is often used to find out the distribution of the first passage time. The algorithm is as below:

1. Simulate the degradation process with Equation [2.2](#) for wiener process and Equation [2.3](#) for Geometric Brownian motion.
2. The process is stopped when the degradation level reaches the threshold.
3. Record the time  $T$  when the process stopped.  $T$  is the first passage time for the process.
4. Start a new degradation process from initial state and repeat step 2 and 3.
5. Use the recorded time to get the CDF of the first passage time.

The algorithm is normally easy to implement. And the process shall be repeated as many as possible to make the result approaching the truth. However, the uncertainty of result can not be avoid since the whole process are randomly simulated. Therefore, it normally only be picked up when there is no other good methods or to verify the results from others.

**2.4 Digital Twin**

The term of Digital Twin is first introduced by Grieves, Michael during his course on Product Life-cycle Management (PLM) in University of Michigan in 2003 [Grieves \(2014\)](#). He has implemented the concept in several projects and consider Digital Twin as the fundamental of next generation of problem solving and innovation. He believes that Digital Twin could help to improve productivity, uniformity of production and improve products quality by focusing on connection of physical product and the virtual product.

There are various definitions about digital twin given by [Grieves \(2014\)](#), [Glaessgen & Stargel \(2012\)](#), [Lee et al. \(2013\)](#), [Erikstad \(2017\)](#), [Saddik \(2018\)](#) and [Tao et al. \(2019\)](#). A common understanding about Digital Twin is that it contains three parts which are physical part, virtual part and connections between these two parts. The connection parts are often called the Digital Thread. As time goes by, the Digital Twin starts to be defined as a real-time modeling. The properties of physical parts should be reflected in the virtual parts in real-time. And the actions taken in the virtual parts should be implemented in the physical parts at the same time. These properties require the connection between physical parts and virtual parts efficient and accurate. The real-time Digital Twins can be used in more areas than the traditional type since it can be used to simulate the real system in computer in parallel. Real-time synchronization is a basic element of Industry 4.0, so digital twin is important in the modern industry. [Vatn \(2018\)](#) clarifies basic terms and give example for the real-time synchronization of operation and maintenance in Industry 4.0. It is also possible to have a digital prototype instead of physical one to save cost and money in design stage. For system with limited access, it is more easy to monitor the system status and to take actions through the internet.

In the other hand, the virtual part is not necessary to copy all the properties of the physical part. It is perfect to have the whole picture of the physical part in virtual part, but there are so many constraints when the model is built up such as computer capabilities, lacking information, speed limitation for synchronize and analysis. Hence the model should be simplified to the properties which are critical and influencing the final decisions. Then it gives more freedom to model systems and to focus more on the critical parts. In addition, it helps to reduce the complexities of system and then makes it less challenging for models building up and maintenance. It also makes the usage of computer capabilities more efficient and cost friendly. Therefore, it is important to find the balance of how reality shall the virtual part to be built.

Furthermore, digital twin models are created based on either physical models or data-driven models. According to the literature review in the specialization project, for the resources reviewed within maintenance and digital twin area, all the models mentioned are data-driven models. For example, fault diagnosis model from [Xu et al. \(2019\)](#) and [Gitelman et al. \(2019\)](#), status monitor models from [Tahmasebinia et al. \(2019\)](#) and [Omer et al. \(2019\)](#). The resources suggest the steps for Digital Twin model of maintenance as below:

- To create a maintenance model based on data collected
- To build the virtual part reflecting the data model properties
- To make connection between these two parts.

The Digital Twin can help to visualize results of traditional maintenance model and simulate the model results to make a better maintenance plan. In addition, the digital twin can be used in real time for control and decision purposes.

# Chapter 3

## RAMS Experiments of Bearing Degradation

The experiment is part of a PhD project which started in Autumn of 2019 and can be treated as two stages up to now. The first stage is in autumn semester of 2019. The equipment is settled by Mr. Viggo Gabriel Borg Pedersen. And the first two experiments is carried out by PhD student Bahareh Tajiani with instructions from Viggo. The main objective of initial experiment is to test the equipment and software, and decide the experiment process. I joined in the project from February of 2020 which is the second stage of experiment. Then Bahareh and I collaborated on the work. The idea was that one could run several experiments to investigate the relation between explanatory variables and the degradation speed. The procedure for experiment are settled according to the literature review and experience from the previous experience of Bahareh. The original plan is to run 9 experiments to test bearings in combinations of two stress and three stress level for each stress. While the plan has to be changed due to the COVID-19, only four experiments were carried out for changing one stress with two stress level. Each of us completed 2 experiments. A experiment log form is proposed by me.

### 3.1 Experimental Setup

#### 3.1.1 Preparation of Experiment

The following items are clarified before the start of experiment.

- The purpose of the experiment is to get real degradation data from bearings and to use the data on different maintenance model for better understanding models and estimating related parameters. Because the limitation of time, equipment and testing bearings, the experiment shall try to get more data from the limited times of experiment.

- The responses of experiment is vibration of bearings. It is very common to use acceleration data to observe the degradation trends for bearings. [Bechhoefer Eric \(Oct. 2013\)](#) proposed an online vibration-based diagnosis method for wind turbine high-speed bearing monitoring. The method has been discussed and implemented in the specialization project report last autumn.
- The potential manipulated factors can be Revolutions Per Minute (RPM), quality of lubricant oil (to simulate environment pollution for working bearings), weight on shaft (to simulate the unbalance operating shaft) etc.
- The operating region is on the designed test rig and shall be monitored by people.
- The test shall use the available equipment and testing bearings in the RAMS lab.

### 3.1.2 Test Rig

The bearings are placed in the bearing house of the test rig which is shown as Figure 3.1. The test rig is designed for studying the degradation of bearings in the real world operations with additional plastic covering for protection. The test rig includes an electric motor, a horizontal shaft, two bearing house (The one closed to motor is for test bearing and the other one is for the balance bearing.), four accelerometers mounted on bearing house to collected vibration data vertically and Horizontally.

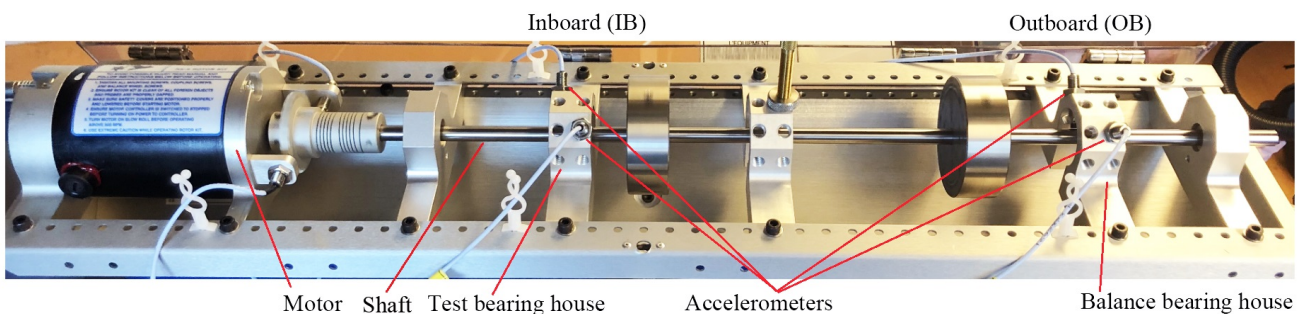


Figure 3.1: Picture of Experiment Setup

### 3.1.3 Bearings

The bearings used for experiments are typical ball bearings which is a type of rolling-element bearing that uses balls to maintain the separation between the bearing races (<https://en.wikipedia>



[.org/wiki/Ball\\_bearing](https://en.wikipedia.org/wiki/Ball_bearing)). The status of bearings are as good as new before the starting of experiment. Expected failure of bearings might be defected inner ring, defected outer ring and defected balls. Specifications of bearings are listed as Table 3.1.

Table 3.1: Specifications of Bearings

Type of Bearing	Open roller/ball bearings
Number of balls	10 Balls
Pitch diameter (B)	70 mm
Ball diameter	4.7 mm
Inner diameter(d)	15.9 mm
Outer diameter(D)	34.9 mm

Note: The bearing in the balance bearing house is always considered as good as new.

### 3.1.4 Accelerometer

The accelerometers are produced by Kistler Group. The type is 8702B100, K-Shear® General Purpose Accelerometer, 25 - 500g. For each bearing house, there are two accelerometers installed. One is on the top to measure the vertical acceleration and the other one is on the right side of bearing house to measure the horizontal data. The locations are shown as Figure 3.2. The location is set according to ISO 10816-7: 2009. It mentions that the measurement locations shall normally be made at each bearing housing in two orthogonal radial directions and possibly one axial direction. (GOST (n.d.))

As discussed by Monitoring (1994), the response of vibration data are different for different orientation of shaft and failure modes. For the horizontal shaft which is same with our experiment, the vibration diagnostic table is shown as Figure 3.3. From the table, it is clear that we need to select different vibration indicators for different failure modes and none indicator works for all failure modes. Therefore, we need to compare all the vibration indicators and to find out which one shall be used. The indicator performance also can help to figure out the failure mode. For the experiment run in RAMS lab, the failure mode is wear-out which does not mentioned in the table. Therefore, all the information shall be compared carefully to find out the most suitable indicator for analysis.

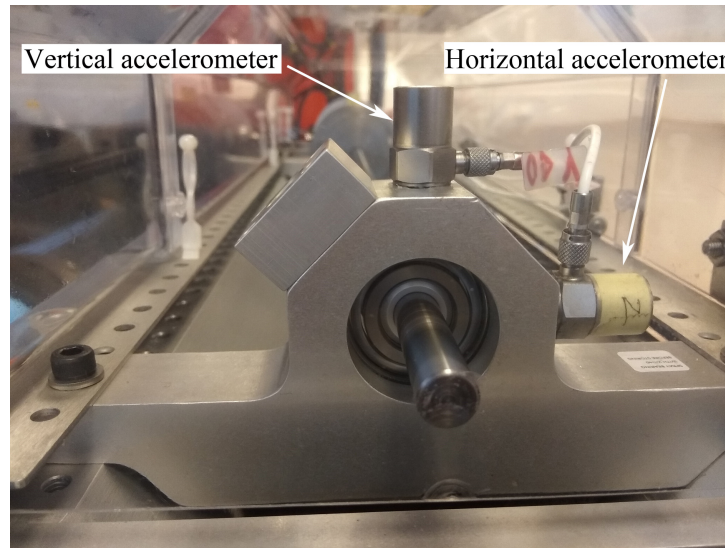


Figure 3.2: Picture of Accelerometer

**ISO 2372 Vibration Diagnostic Table  
(Horizontal Shaft)**

	Excessive Horizontal	Excessive Vertical	Excessive Axial	Excessive Structural	Notes
	Vibration Indicates:	Vibration Indicates:	Vibration Indicates:	Vibration Indicates:	
<b>Imbalance</b>	YES	NO	NO	NO	Horizontal > Axial
<b>Misalignment</b>	NO	YES	YES	NO	Axial > Horizontal
<b>Looseness</b>	YES	YES	NO	YES	Vertical ≥ Horizontal
<b>Electrical Faults Measured as Vibration</b>					To detect an electrical problem:  Turn off machine power and monitor vibration. If the vibration immediately drops, the problem is electrical.

**Note:** On an overhung machine, imbalance and misalignment may display similar characteristics. Use phase measurements to differentiate between the two.

**Note:** YES = ISO 2372 Unsatisfactory – Unacceptable Levels.

NO = ISO 2372 Good – Satisfactory Levels.

Figure 3.3: ISO 2372 Vibration Diagnostic Table

### 3.1.5 Amplifier

The system contains a coupler produced by Kistler Group. It is a 4-Channel TEDS Piezotron (IEPE) Coupler with display. Type is 5134B. The 4-channel TEDS Piezotron (IEPE) coupler is suitable for the operation of Piezotron (IEPE) sensors: Adjustable gain of 0.5... 150 in 0.01 increments USB 2.0 interface IEEE 1451.4 (TEDS-compatible) LEDs for status display Selectable time constants and supply current (Resource refer to <https://www.kistler.com/en/product/type>

-5134b/). The coupler amplified the acceleration data to make the features more significant for further analysis.



Figure 3.4: 4-Channel TEDS Piezotron (IEPE) Coupler with display

### 3.1.6 Software

The software system is provided by Bently Nevada which is an asset protection and condition monitoring hardware, software and service company (Bently (2020)). The system could monitor the vibration data of bearings on frequency domain and time domain in real-time. Display window can be set up as needed. Figure 3.5 shows an example of the monitor. However, data has to be saved manually which means data are discrete and there is uncertainty about the time interval. Finally, Mathwork's Matlab R2019b software was used for further analysis of the data. The analysis was a preliminary assessment of trends in the data.

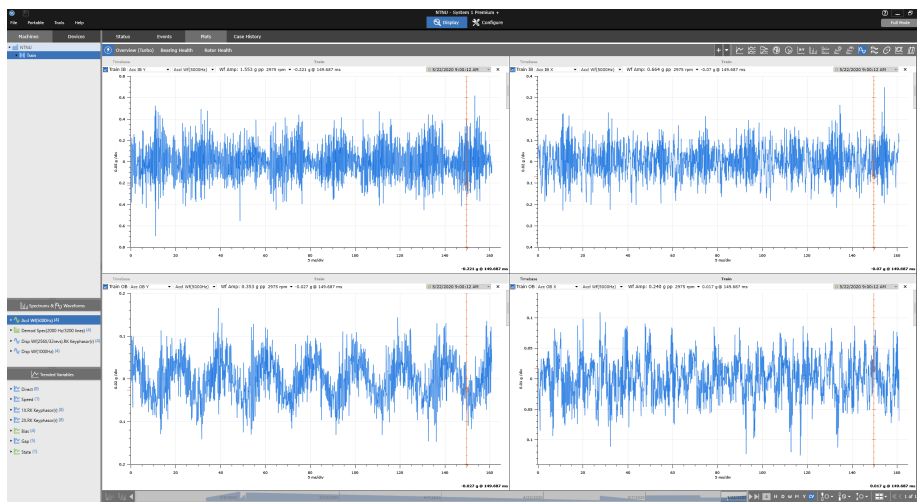


Figure 3.5: System working Page

### 3.1.7 Considered factors

There are many factors which can cause bearing failure, such as improper lubrication, contamination, overload, high or low operating temperatures, and improper handling and installation (Refers to <https://www.flowcontrolnetwork.com/home/article/15563223/causes-effects-and-prevention-of-bearing-failures>). While there is no information about the bearing designed rated load such as natural frequency, maximum speed and temperature, these factors shall be controlled within the normal operation region to avoid their affects. Then factors manipulated in the experiment could be RPM, lubrication, contamination, external force which can assume caused by improper installation and weight on shaft which to simulate the unbalanced operation.

The first factor considered is RPM. It can be controlled by a speed control kit which can adjust the rotation speed from 0 ~ 5000 RPM.

The second factor considered is contaminated lube oil. Silicon carbide is selected as the contamination of lube oil. This can simulate bearings working in dirty place or used bad quality lube oil. The size silicon carbide and density of mixture are the factors which can be controlled manually to keep the stress constant or increased steadily. Since the hardness of silicon carbide is 9.5 on the Mohs hardness scale (Ploszajski (2016)), the size of silicon carbide is assumed no change during the bearing operation but the amount of silicon carbide inside bearing might reduce due to high speed rotation of bearing. The frequency of adding mixture shall be discussed and controlled carefully after more information received from experiment.

The Third factor considered can be external force on bearings. It can cause bearings running unbalanced and failed earlier. The external force shall be stable since it normally caused by improper installation and shall not change intensity or direction frequently. The intensity of external force can controlled manually in different level. However, additional equipment is required to have the external force.

The experiment shall be operated in a safe manner which means testing shall run within the limitation of all equipment such as the capability of motor, accelerator meter and shaft. And the testing shall be stopped immediately whenever there is high temperature, abnormal noise or high vibration of structures.

## 3.2 Experiment Procedure

### 3.2.1 Overview

As mentioned, PhD student Bahareh Tajiani completed the first two experiments with instructions from Viggo. The termination condition is 10 g for the absolute value of Vertical acceleration data. And the analysis region is time domain. Both the first two experiments set motor speed around 3000 RPM and added lube oil which mixed the smallest size of silicon carbide once an hour.

The second stage of experiments planned to start in beginning of Spring semester 2020. The original plan is to have two stress which are motor speed and silicon carbide. It can be set as three levels for each stress. For motor speed, the stress level could be 2000 RPM, 3000RPM and 4000RPM. For silicon carbide, the stress level could be size of silicon carbide or frequency of adding silicon carbide. According to factorial design theory mentioned in Section 2.2.1, the minimum time of experiment shall be  $n^k = 2^3 = 9$  times, if both stress has three stress levels. However, due to the COVID-19, the second stage of experiment cannot start until end of May 2020. Finally, there are only four experiments carried out with same amount of mixed lube oil and different motor speed. The 3<sup>th</sup> and 4<sup>th</sup> experiments are ignored since amplifier was not connected. Therefore, the 2<sup>nd</sup>, 5<sup>th</sup> and 6<sup>th</sup> experiment are used for analysis.

### 3.2.2 Procedure

The procedure of the experiment is listed as below

1. Place tested bearing in the test bearing house;
2. Check all equipment are connected and powered properly;
3. Switch on the rotor control kit and then the bearing starts to operate. Set the speed as designed;
4. Open the management software 'System 1', login with NTNU account;
5. Set up the monitor page and turn the status to CV (current value) to have the on-line plots;
6. Wait the rotor speed constant and start to add lube oil mixture. The frequency is 2 spatter every 10 samples (the frequency changed to 1 spatter every 5 samples from the second stage of experiment);

7. Save vibration data every 6 minutes (Time interval changed to 5 minutes from the second stage of experiment);
8. For the first stage of experiment, vertical acceleration data are recorded. For the second stage of experiment, both vertical and horizontal acceleration data are saved.
9. When the level of noise larger than 80 dB, check the maximum value of absolute vertical vibration value, stop the experiment when it exceeds 10 g.

Note: Since the experiment may involve more than one person, a form for experiment information record is proposed as Appendix B. The form includes information about all settings during experiment such as stress levels, changing log, data set time, file name etc.

### 3.2.3 Data Storage and Feature Extraction

The vibration data shall be saved manually as 'csv' file. Each file contains following information:

- Sample speed;
- Record time information;
- X-Axis is time;
- Y-Axis is acceleration data at time of X-Axis;
- Each file contains vibration data of eight circles;
- The time step in the file is 0.078 ms (millisecond). Therefore, duration of each data set is from 150 to 250 ms , depends on the rotor speed.

# Chapter 4

## Case Study for the First Passage Time

Before implementing the first passage time models with the experiment data, the methods shall be verified with typical stochastic differential equations. Parameters are assumed according to Wiener process and Geometric Brownian motion's definitions. The threshold is set as fixed values. Then all three methods for the first passage time are implemented with those parameters. This is the preparation before using the methods on real experiment data.

### 4.1 Wiener Process

Firstly, SDE is selected as Wiener process. Then the first passage time can be calculated with methods Inverse Gaussian distribution function, Numerical integration, and Monte Carlo simulation respectively.

The initial state are setup as below.

- Initial state  $W(0) = 0$ ;
- Threshold  $L = 50$ ;
- Drift parameter  $\mu = 1$ ;
- Infinitesimal parameter  $\sigma = 0.4$ . Note in Equation 2.23, we need to calculate  $e^{2\lambda/v}$ , then  $\sigma$  should be set larger than 0.4, otherwise the value of  $e^{2\lambda/v}$  will be too large to calculate. This does not mean the function is incorrect, but the capacity of the computer calculation.

#### 4.1.1 Inverse Gaussian Distribution function

As discussed in Section 2.3.1, the first passage time of Wiener process follows Inverse Gaussian distribution and can be calculated with function 2.23 directly. The method is straight forward.

The mean value and variance can be calculated with Equation 2.25 and 2.26 as below

$$E(T) = v = \frac{L}{\mu} = \frac{50}{1} = 50 \quad (4.1)$$

$$Var(T) = \frac{v^3}{\lambda} = \frac{L\sigma^2}{\mu^3} = \frac{50 * 0.4^2}{1^3} = 8 \quad (4.2)$$

The CDF and PDF of the first passage time is shown as Figure 4.1.

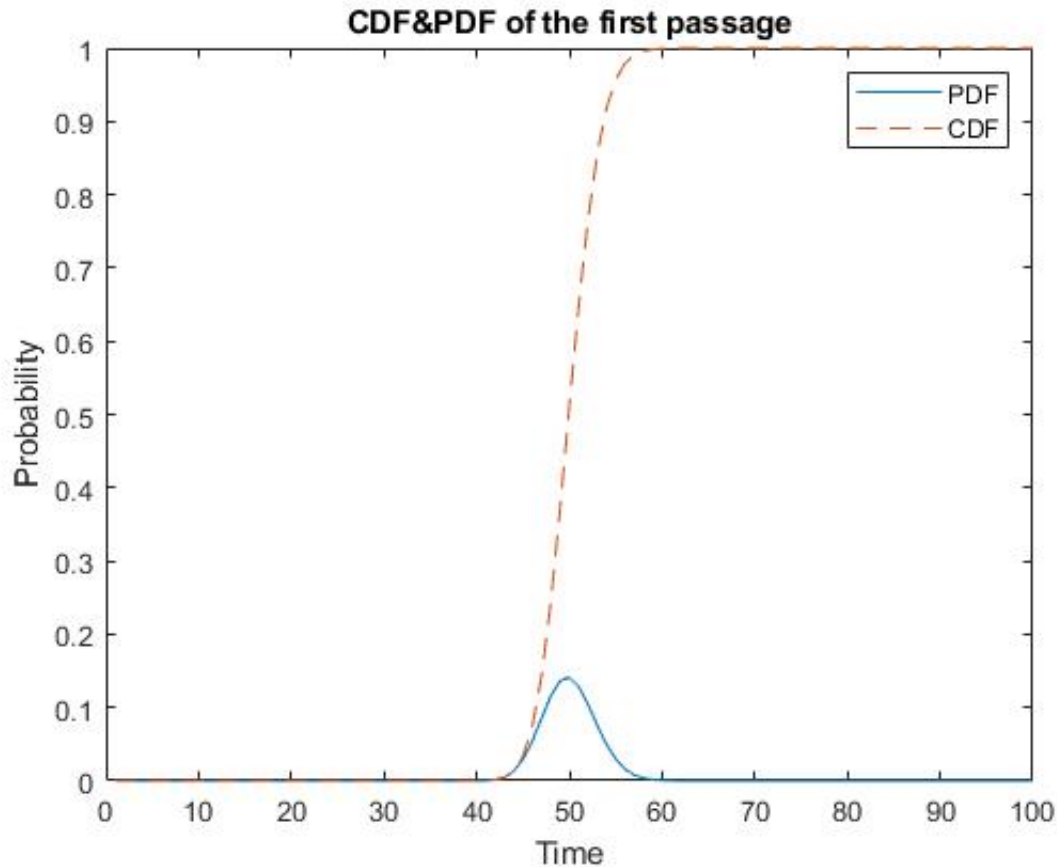


Figure 4.1: CDF and PDF of the first passage time by Inverse Gaussian distribution

### 4.1.2 Numerical integration

As discussed in Section 2.3.2, the PDF of each increment can be calculated. In the study case, the detail process is as below.

- The initial state is  $W(0) = 0$  and  $t = 0$  which means  $f(0 | t = 0) = 1$  and  $f(y_i | t = 0) = 0$  if  $y_i \neq 0$ .



- So the first increment must start from 0 and the time interval is  $dt$ .
- The PDF of the increment  $g(s)$  is normal distribution with parameter  $\mu' = \mu * dt$  and  $\sigma' = \sigma * \sqrt{dt}$ .
- Therefore, with Equation 2.31, we have

$$f(y|0+dt) = \int_{y-L}^{\infty} f(y-s|t=0)g(s)ds = g(s) \quad (4.3)$$

- From the second increment, Equation 2.33 shall be implemented with the result of  $f(y_i | t)$  from previous steps.
- The foot print of PDF of increment becomes larger and maximum value becomes smaller with the integration.
- The process stops when the maximum value of PDF is very Small compared with the initial maximum value.
- The results of PDF of deterioration level at time  $t + dt$  is shown as Figure 4.2.

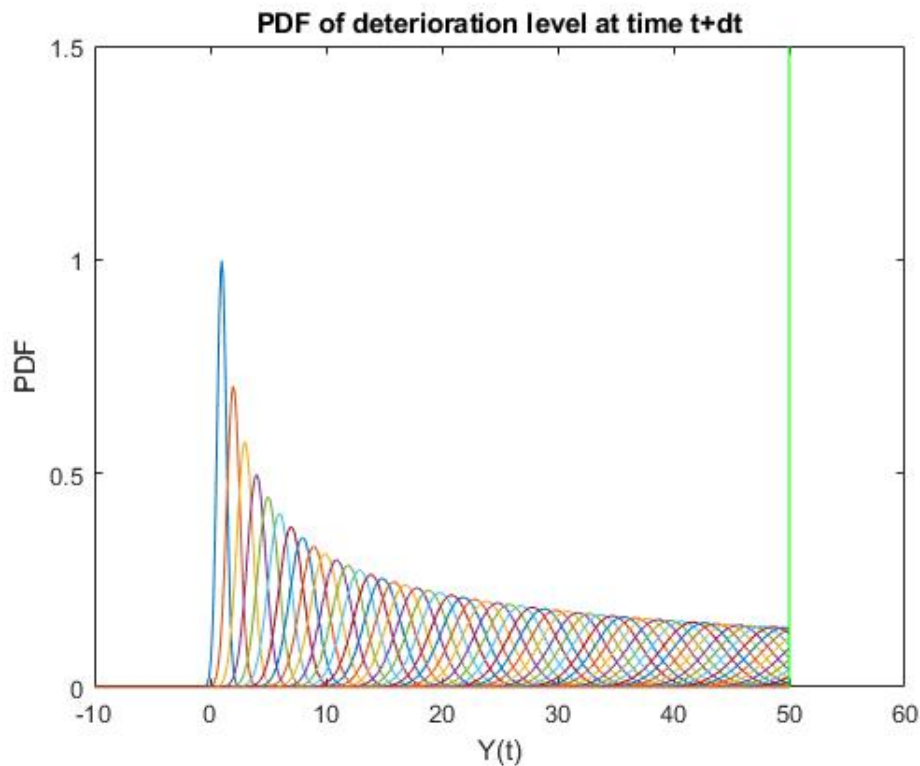


Figure 4.2: PDF of the first passage time by Integration

- Then we can use Equation 2.32 to get the CDF of the first passage time.  $F_T(t) = Pr(T \leq t) = 1 - \int_{-\infty}^L f(y | t) dy$
- The plot is shown as Figure 4.3.

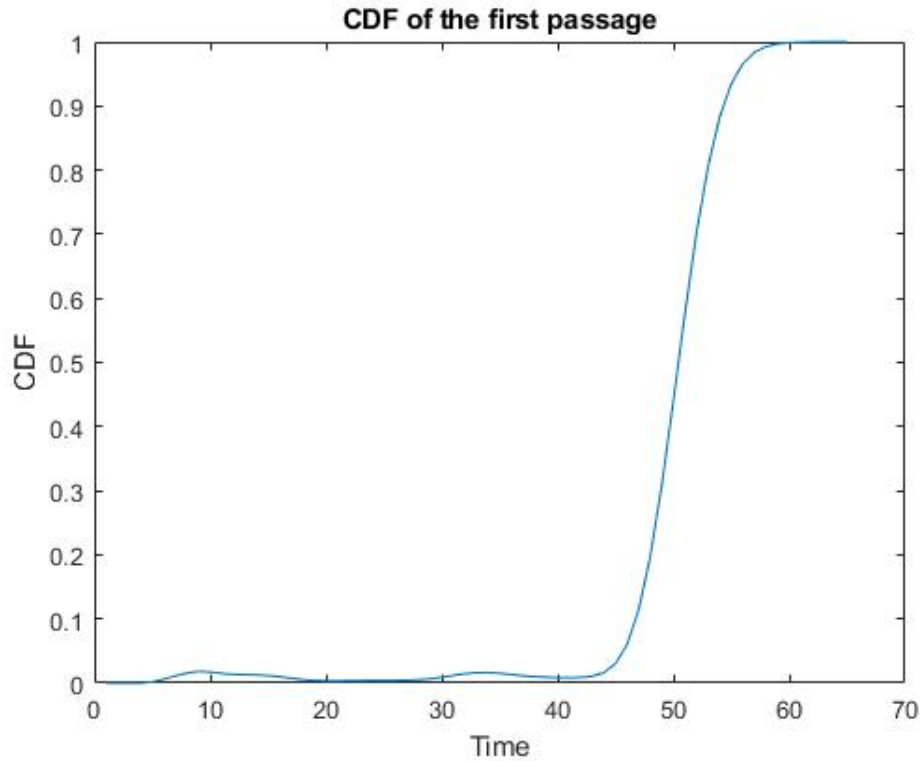


Figure 4.3: CDF of the first passage time by Integration

- Then the PDF of the first passage time is  $f(t) = F(t+1) - F(t)$ .
- Mean value of the first passage time  $E(T) = 50.6288$ .
- Variance of the first passage time  $Var(T) = 3.228$ .

### 4.1.3 Monte Carlo simulation

Now Monte Carlo is introduced to simulate the degradation process and verify the result obtained from previous methods.

The algorithms is as below:

1. Assume the initial state  $Y = 0$ ;

2. Use computer to simulate each random jump at  $dt$ . They follows normal distribution when  $dt$  is unchanged. Parameter are given with Equation 2.2.
3. If the progress reaches the limit after one jump, the passage time  $T$  and value of  $Y$  shall be recorded and the process stops increasing.
4. Start a new progress from initial state and repeat step 2 & 3.
5. Quit the whole loop when it has enough data.
6. Statistic and make histogram to find out the PDF and CDF of the first passage time.

**Note:** The simulation number shall be large to get enough data for analysis. It is 50000 times for the example.

- The result of simulated data is shown as Figure 4.4, 4.5 and 4.6.
- Mean value of the first passage time  $E(T) = 50.1164$ .
- Variance of the first passage time  $Var(T) = 7.9970$ .

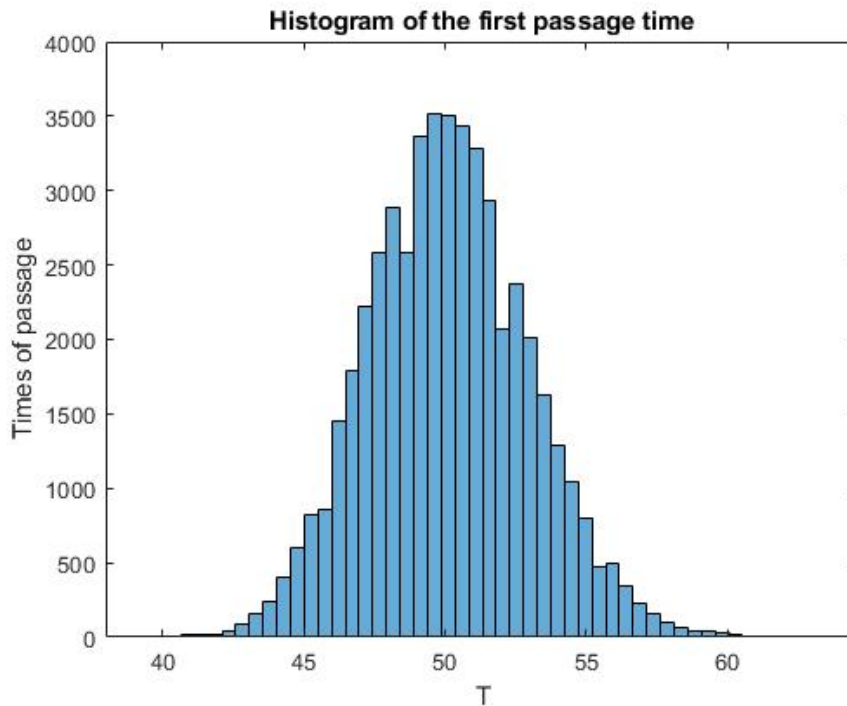


Figure 4.4: Histogram of the first passage time by Simulation

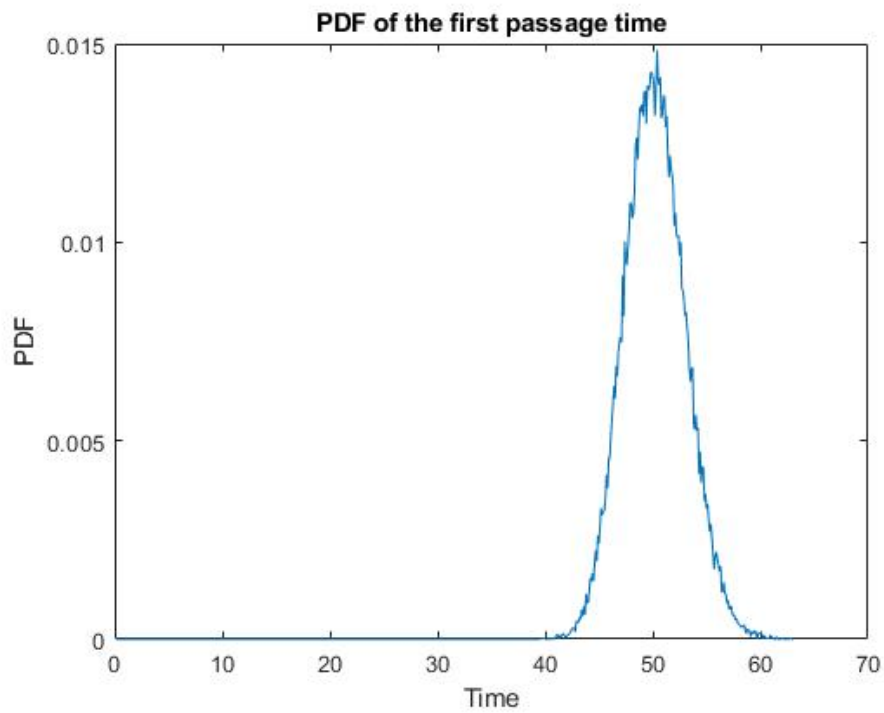


Figure 4.5: PDF of the first passage time by Simulation

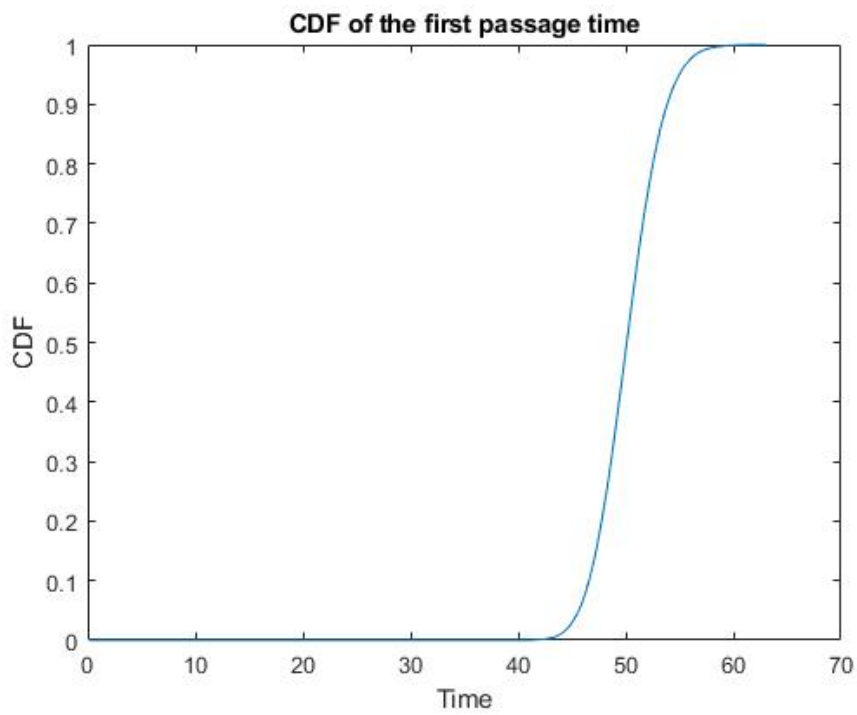


Figure 4.6: CDF of the first passage time by Simulation

#### 4.1.4 Brief Summary

Comparing Figures 4.1, 4.3 and 4.6. The results are similar with each other especially the plots of Inverse Gaussian distribution and Monte Carlo simulation. This means these methods are equivalent when they are used to calculate the CDF of the first passage time. In addition, these methods can prove each other, and possess the characteristics of their own at the same time. The expected value  $E(T)$  and variance  $Var(T)$  are listed as Table 4.1 for these methods .

Table 4.1: Results of the First Passage Time for Wiener Process

Method	$E(T)$	$Var(T)$
Inverse Gaussian Distribution	50	8.0
Integration	50.6288	3.228
Monte Carlo simulation	50.1164	7.9970

From above table, there are some findings as below

- Inverse Gaussian distribution is the most rough methods which has the highest variance value.
- But the result from Inverse Gaussian distribution is constant when parameters are fixed and it is the easiest method to be implemented.
- Integration methods has the least variance and the process could help us to understand the distribution while degradation.
- From Figure 4.5 of Monto Carlo simulation, the plot is not as smoothing as other methods, more simulation round shall be used to get better results.
- The expected value  $E(T)$  from Monto Carlo simulation is varying every time since the process is simulated randomly. Therefore, the result is not very reliable.

## 4.2 Geometric Brownian motion (GBM)

Now GBM is selected as the SDE used for finding the CDF of the first passage time. As discussed in Section 2.1.2, GBM is normal distributed and exponential distributed. Both of them will be discussed within the case study. For easy comparison, the parameters are similar with Wiener process and set up as below.

- Initial state  $S(0) = 0.1$ . (It cannot equal to 0);
- Threshold  $L = 50$ ;
- Drift parameter  $\mu = 1$ ;
- Infinitesimal parameter  $\sigma = 0.4$ .

### 4.2.1 Inverse Gaussian Distribution function

The method is similar with Wiener process, which is also using Equation 2.23, where  $v = \frac{\log L - \log S_0}{\mu - \frac{1}{2}\sigma^2}$  and  $\lambda = \frac{(\log L - \log S_0)^2}{\sigma^2}$ . The method is straight forward. The mean value and variance can be calculated with Equation 2.28 and 2.29 as below.

$$\begin{aligned} E(T) &= v = \frac{\log L - \log S_0}{\mu - \frac{1}{2}\sigma^2} \\ &= \frac{\log(50) - \log(0.1)}{1 - \frac{1}{2} * 0.4^2} = 6.7550 \end{aligned} \quad (4.4)$$

$$\begin{aligned} Var(T) &= \frac{v^3}{\lambda} = \frac{\sigma^2(\log L - \log S_0)}{(\mu - \frac{1}{2}\sigma^2)^3} \\ &= \frac{0.4^2 * (\log(50) - \log(0.1))}{(1 - \frac{1}{2} * 0.4^2)^3} = 1.2769 \end{aligned} \quad (4.5)$$

The CDF and PDF of the first passage time is shown as Figure 4.7.

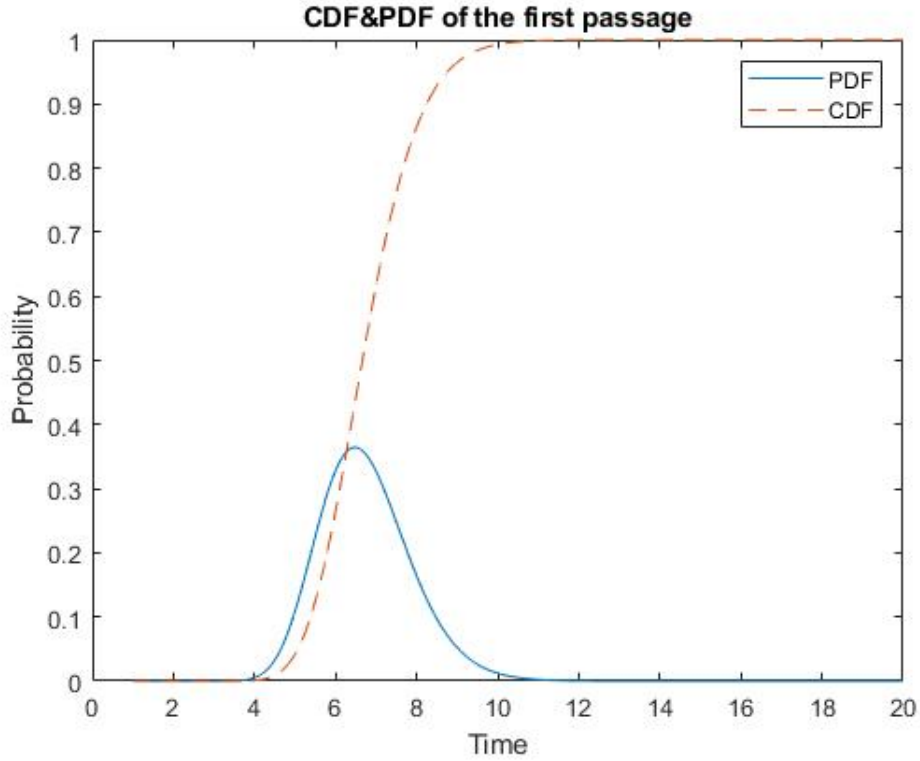


Figure 4.7: CDF & PDF of the first passage time by Inverse Gaussian distribution

## 4.2.2 Numerical integration

As discussed in Section 2.3.2, the method is to calculate PDF of all increments with time interval  $dt$  and then use Equation 2.32 to get the CDF of the first passage time. Unlike Wiener process, the distribution of each increment for GBM is related to both time interval and the current status. Therefore, Equation 2.31 shall be rewritten as below.

$$f(y | t + dt) = \int_{y-L}^{\infty} f(y-s | t) g(s | y-s) ds \quad (4.6)$$

where  $f(y-s | t)$  can be obtained from last integration result and  $g(s | y-s)$  is the PDF of normal distribution with parameters: mean value  $\hat{\mu} = \mu(y-s)dt$  and variance  $\hat{\sigma}^2 = \sigma^2(y-s)^2 dt$ .  $y$  value is changed with loop  $i$  from  $f(i | t)$  to  $f(i+1 | t)$ , and  $s$  is changed together with loop  $j$  from  $jdy$  to  $(j+1)dy$  in the integration.

The detail process is as below:

- The initial state is  $S(0) = 0.1$  and  $t = 0$  which means  $f(0.1 | t = 0) = 1$  and  $f(y_i | t = 0) = 0$  if  $y_i \neq 0.1$ .
- The first increment must start from 0.1 and the time interval is  $dt$ .

- Therefore, with Equation 4.6, we have

$$f(y|0+dt) = \int_{y-L}^{\infty} f(y-s|t=0)g(s|y-s)ds = g(s|y-s) \quad (4.7)$$

- According to Equation 2.3, the PDF of the increment  $g(s|y-s)$  is normally distributed with parameters  $\hat{\mu} = \mu(y-s)dt$  and  $\hat{\sigma} = \sigma(y-s)\sqrt{dt}$ .
- For the first increment, the parameter for the normal distribution shall add the initial state, then the mean value is  $S_0 + S_0 * \mu dt$ , the variance is  $\sigma^2 S_0^2 dt$ . In the other hand, we can also use log-normal distribution as described by Equation 2.6 in Section 2.1.2. Then the mean value is  $\log(S_0) + (\mu - \frac{\sigma^2}{2})t$  and variance is  $\sigma^2 t$ . Since it is the first increment,  $t = dt$ .
- The following steps are same with wiener process which refer to Section 4.1.2.
- The results of PDF of deterioration level at time  $t + dt$  is shown as Figure 4.8.

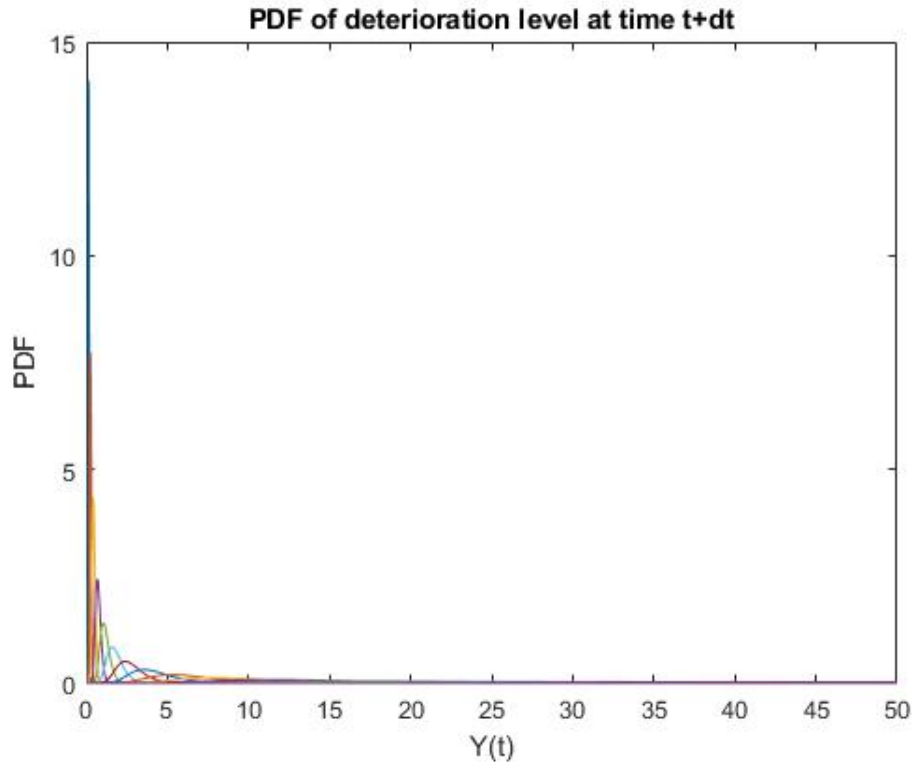


Figure 4.8: PDF of each Degradation by Integration

- The plot of CDF of the first passage time is shown as Figure 4.9. (All use normal distribution.) The plot is not very smoothing, smaller  $dt$  and  $dy$  shall be used to improve the



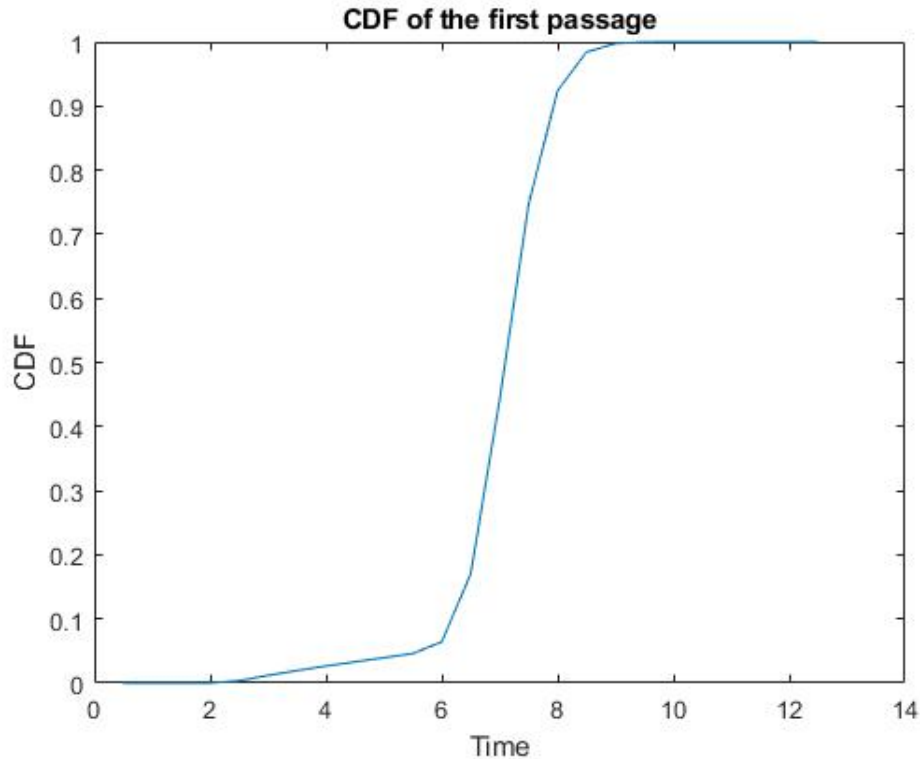


Figure 4.9: CDF of the first passage time by Integration

result which will increase the complexity of calculation and cost much more time to reach result.

- Then Mean value of the first passage time is  $E(T) = 7.2456$  (The first  $dt$  is normal distributed.) and  $E(T) = 7.1787$  (The first  $dt$  is log-normal distributed.).
- Variance of the first passage time is  $Var(T) = 0.3971$  (The first  $dt$  is normal distributed.) and  $Var(T) = 0.3715$  (The first  $dt$  is log-normal distributed.).

### 4.2.3 Monte Carlo simulation

The algorithms is similar with wiener process while the initial state is  $S(0) = 0.1$ . Here we use both normal distribution of Equation 2.3 and log-normal distribution of Equation 2.6 to simulate the degradation process respectively.

For the normal distribution whose mean value is  $\mu(y-s)dt$  and variance is  $\sigma^2(y-s)^2dt$ . The results are shown as Figure 4.10, 4.11 and 4.12.

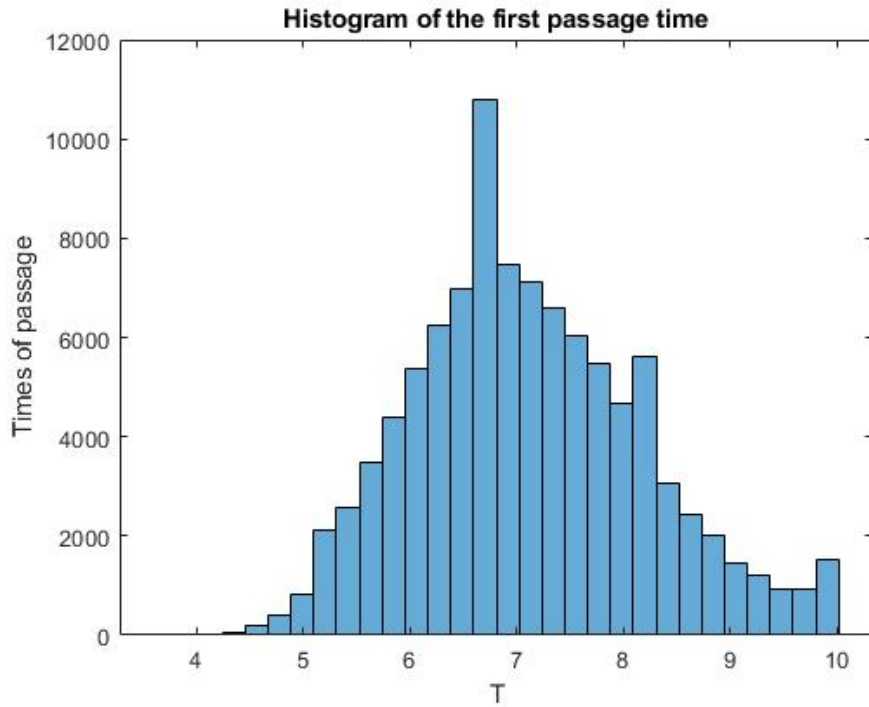


Figure 4.10: Histogram of the first passage time by Monte Carlo simulation

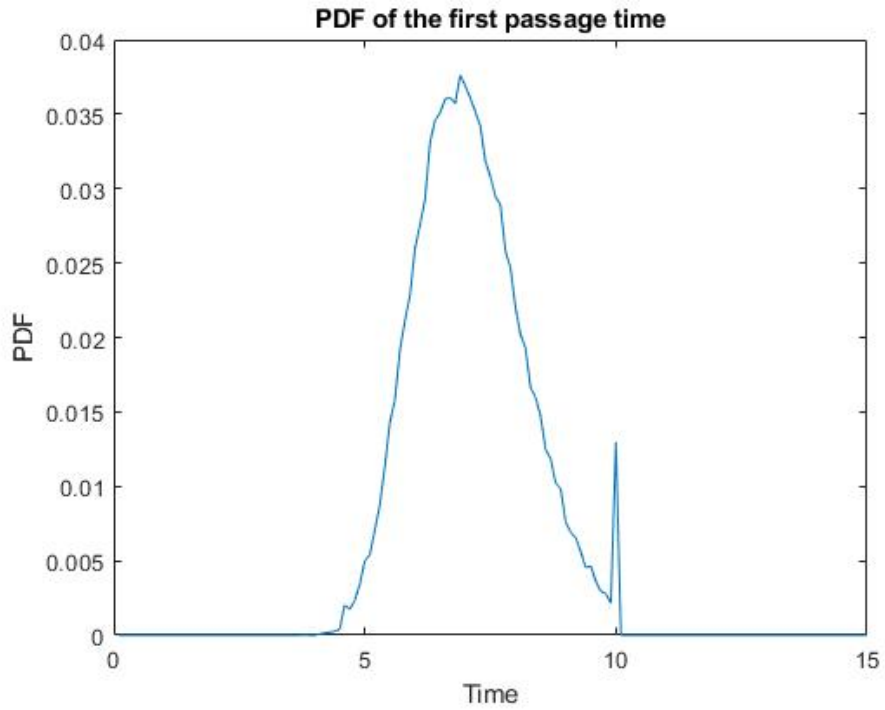


Figure 4.11: PDF of the first passage time by Monte Carlo simulation

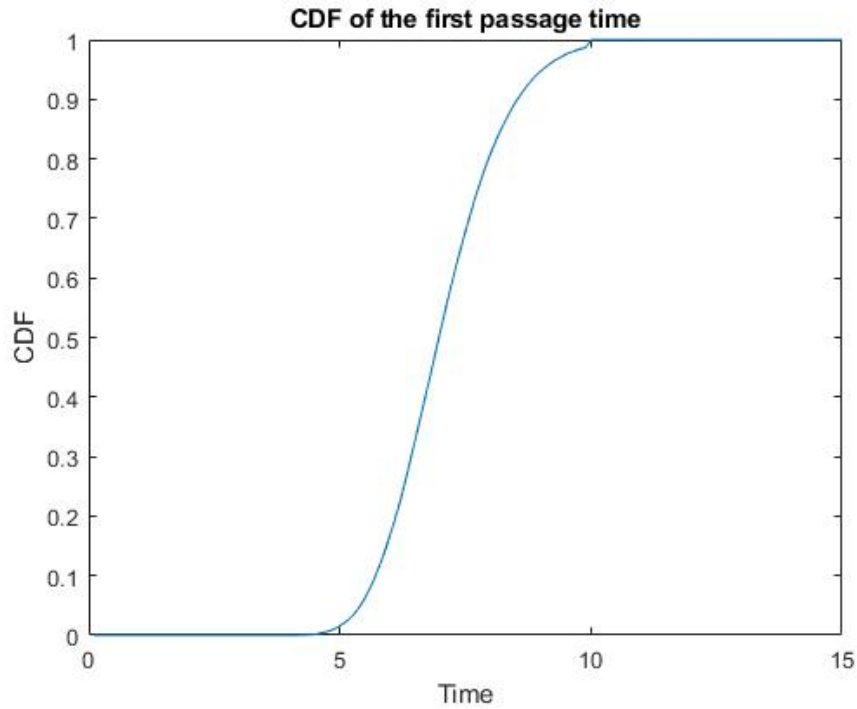


Figure 4.12: CDF of the first passage time by Monte Carlo simulation

- Mean value of the first passage time  $E(T) = 7.1116$ .
- Variance of the first passage time  $Var(T) = 1.1938$ .

For the log-normal distribution whose mean value is  $\log S_0 + (\mu - \frac{\sigma^2}{2}) * t = \log(0.1) + (1 - \frac{0.4^2}{2}) * t = -2.3026 - 0.92t$  and variance is  $\sigma^2 t = 0.4^2 * t = 0.16t$ .

- Mean value of the first passage time  $E(T) = 6.8588$ .
- Variance of the first passage time  $Var(T) = 1.2605$ .
- The plots are shown as Figure 4.13, 4.14 and 4.15 which are different with normal distribution's plots.

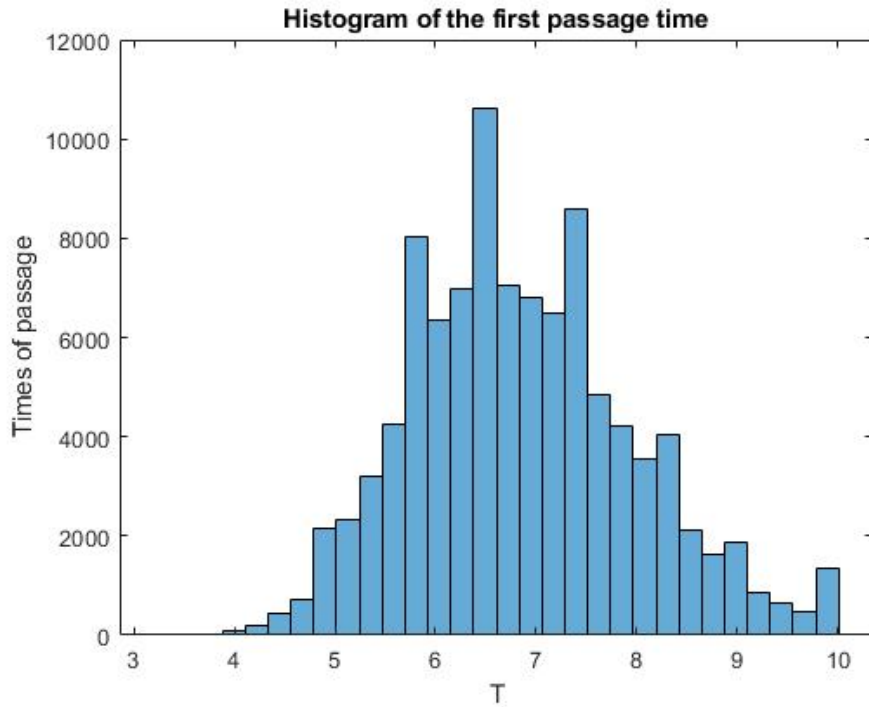


Figure 4.13: Histogram of the first passage time by Monte Carlo simulation

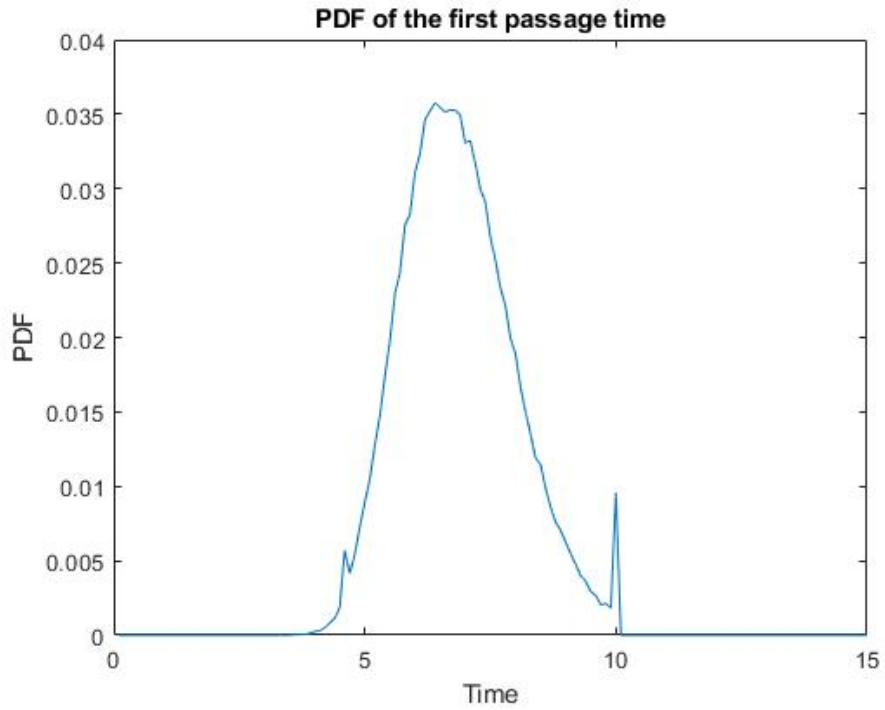


Figure 4.14: PDF of the first passage time by Monte Carlo simulation

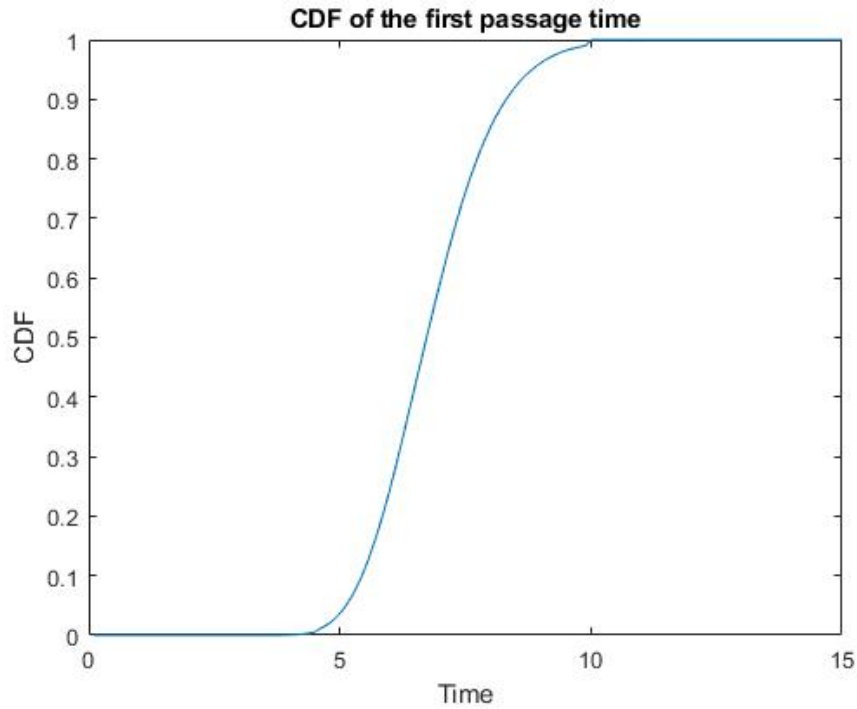


Figure 4.15: CDF of the first passage time by Monte Carlo simulation

#### 4.2.4 Brief Summary

Comparing Figures 4.7, 4.9, 4.12 and 4.15. The plots are similar with each other especially the result from Inverse Gaussian distribution and Monte Carlo simulation. It is same with wiener process, these methods can prove each other and are equivalent when they are used to calculate the CDF of the first passage time. The expected value  $E(T)$  and variance  $Var(T)$  are listed as Table 4.2.

Method	Distribution increments	$E(T)$	$Var(T)$
Inverse Gaussian Distribution	log-normal distribution	6.7550	1.2769
	Normal distribution	7.2456	0.3971
Integration	log-Normal distribution	7.1787	0.3715
	Normal distribution	7.1116	1.1938
Monte Carlo simulation	log-normal distribution	6.8588	1.2605

From above table, there are some findings as below:

- Most of the findings are similar with Wiener process, it is because the progress for each method is similar with different SDE.
- Inverse Gaussian distribution is still the most rough methods which has the highest variance value.
- The results from Inverse Gaussian distribution is constant when parameters are fixed and it is the easiest method to be implemented. But only log-normal distribution is used for this method.
- Log-normal distribution definition is implemented on all three methods. But normal distribution definition cannot be used in Inverse Gaussian distribution method.
- Integration methods has the least variance for both normal distribution and log-normal distribution.
- The expected value  $E(T)$  from Monto Carlo simulation is different every time since the process is simulated randomly. Therefore, the result is not very reliable.
- The results are different if different definition of GBM is used but similar when definition is same. This means the affects from definition is larger than the affects caused by methods.
- For integration method, the mean value of both definition are closed to each other. That is because the log-normal distribution is only used in the first increment.
- The mean value used log-normal distribution is always smaller than normal distribution which means the degradation process is faster when it is log-normal distributed.

# Chapter 5

## Results

The results from experiment are present within this Chapter. And experiment data is processed by designed models. There are two models discussed in this section. The first one is the first passage time model through methods verified in Chapter 4. The second model is digital twin model which was used in the Specialization project report in Autumn semester of 2019.

### 5.1 Results of Experiment

The vibration data of the 1<sup>st</sup> experiment is plot as Figure 5.1.

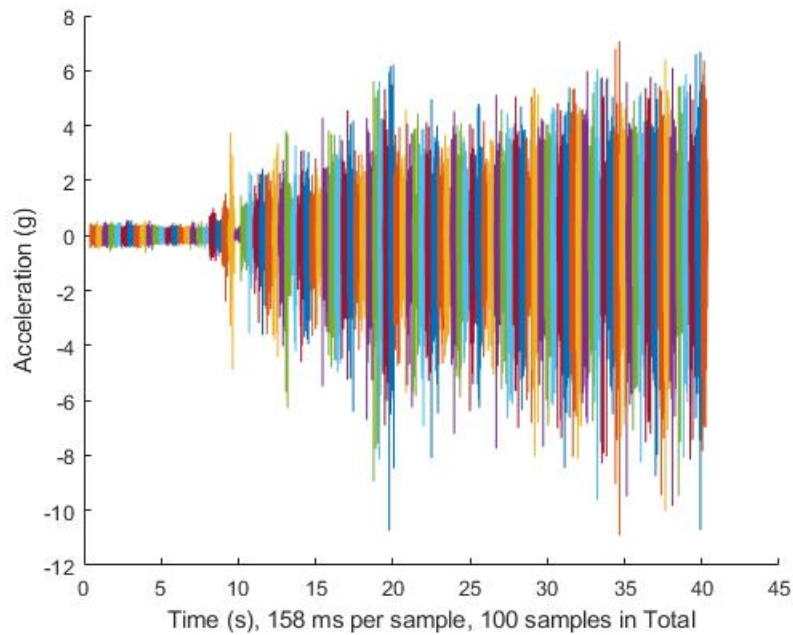


Figure 5.1: The vibration signals in time domain

The vibration signals in time domain reveals an increasing trend of the signal. From the plot, it is clear that the maximum amplitude is negative number, therefore, absolute values shall be used. In addition, the beginning part of data are smoothing because there is no lube oil mixture added during this period.

### 5.1.1 Feature Selection

The statistical features mentioned in [Saidi et al. \(2017\)](#) and [Ali et al. \(2018\)](#) are extracted from time-domain signal. The features' function are listed as Table 5.1.

Table 5.1: Expression and Matlab Function for Features

Feature	Expression	Matlab Fuction
Mean	$\frac{1}{N} \sum_{i=1}^N x_i$	mean(v)
Standard deviation (Std)	$\left( \frac{1}{N} \sum_{i=1}^N (x_i - mean)^2 \right)^{\frac{1}{2}}$	std(v)
Skewness	$\frac{1}{N} \cdot \sum_{i=1}^N \frac{(x_i - \bar{x})^3}{\rho^3}$	skewness(v)
Kurtosis	$\frac{\frac{1}{N} \cdot \sum_{i=1}^N (x_i - \bar{x})^4}{\left( \frac{1}{N} \cdot \sum_{i=1}^N (x_i - \bar{x})^2 \right)^2}$	kurtosis(v)
Peak to Peak	$x_{max} - x_{min}$	peak2peak(v)
RMS (Root Mean Square)	$\left( \frac{1}{N} \sum_{i=1}^N x_i^2 \right)^{\frac{1}{2}}$	rms(v)
CrestFactor	$\frac{x_{max}}{RMS}$	max(v)/features.RMS
ShapeFactor	$\frac{RMS}{\frac{1}{N} \sum_{i=1}^N  x_i }$	features.RMS/mean(abs(v))
ImpulseFactor	$\frac{x_{max}}{\frac{1}{N} \sum_{i=1}^N  x_i }$	max(v)/mean(abs(v))
MarginFactor	$\frac{x_{max}}{\left( \frac{1}{N} \sum_{i=1}^N  x_i  \right)^2}$	max(v)/mean(abs(v))^2
Energy	$\sum_{i=1}^N x_i^2$	sum(v.^2)
Absolute Maximum	$ x_{max} $	abs(max(v))

To select the suitable features for further analysis, the importance of features shall be ranked. [Coble \(2010\)](#) proposes three metrics to quantify the indicators which are trendability (Equation 5.1), monotonicity (Equation 5.2), and prognosability (Equation 5.3). Monotonicity is an impor-



tant indicator of a degradation model since the bearing fault is an irreversible process. Then it is used in the thesis to quantify the merit of the features.

$$Trendability = \min(|\text{corrcoef}(x_i, x_j)|); i = 1, 2, \dots, m; j = 1, 2, \dots, m \quad (5.1)$$

$$Monotonicity = \text{mean} \left( \left| \frac{\text{positive}(\text{diff}(x_i)) - \text{negative}(\text{diff}(x_i))}{n-1} \right| \right) \quad (5.2)$$

$$Prognosability = \exp \left( - \frac{\text{std}(\text{failurevalues})}{\text{mean}(|\text{failurevalue} - \text{startingvalue}|)} \right) \quad (5.3)$$

The result of monotonicity of each features is run and listed as Table 5.2 for all four bearings. Standard deviation and RMS has the average highest monotonicity according to the table. Features with average feature importance score larger than 0.3 are selected for the first passage time model in the next section. The selected features are Standard deviation, Peak to Peak, RMS and Energy.

Table 5.2: Result of Feature Importance

Feature	Bearing 1	Bearing 2	Bearing 5	Bearing 6	Average
Mean	0.0505	0.0505	0.0642	0.1009	0.0665
<b>Standard deviation (Std)</b>	0.2323	0.4343	0.6147	0.3945	<b>0.419</b>
Skewness	0.1515	0.0707	0.0459	0.1193	0.0968
Kurtosis	0.2323	0.1515	0.0275	0.0826	0.1235
<b>Peak to Peak</b>	0.3131	0.3333	0.3028	0.3945	<b>0.3359</b>
<b>RMS</b>	0.2323	0.4343	0.6147	0.3945	<b>0.419</b>
CrestFactor	0.1313	0.1717	0.0826	0.0642	0.1125
ShapeFactor	0.1313	0.2121	0.0275	0.1009	0.118
ImpulseFactor	0.1717	0.1919	0.1193	0.0642	0.1368
MarginFactor	0.1313	0.0505	0.5596	0.1927	0.2335
<b>Energy</b>	0.2323	0.4141	0.6147	0.3761	<b>0.4093</b>

According to the experiment procedure, all experiment stopped when the absolute value of acceleration reaches 10 g. Therefore, these four experiment stopped by the samples shown as

Table 5.3.

Tested Bearing	Sample No	Standard Deviation	Peak to Peak	RMS	Energy	Absolute Maximum
Bearing 1	86	0.8738	17.993	0.8736	1550.793	10.918
Bearing 2	92	1.129	17.985	1.1288	2568.593	11.353
Bearing 5	100	2.2434	18.125	2.2429	10382.87	10.062
Bearing 6	93	1.746	21.335	1.7457	9483.535	11.165

However, the result for Bearing 6 cannot be right since the rotating speed is 2000 RPM for Bearing 6 and 3000 RPM for others. It is very strange to have earlier failure with slower rotating speed. In addition, the vertical values has huge gap compared with horizontal value which is abnormal too. Therefore, the tested Bearing 6 is ignored for the following analysis. In another hand, Bearing 1 is ignored since it is the initial testing and the experiment was stopped frequently to find out the termination condition especially in the later stage.

Bearing 2 and Bearing 5 are selected for the following analysis. The plot of Bearing 2 vs Bearing 5 for above mentioned features are shown as Figure 5.2, 5.3, 5.4 and 5.5.

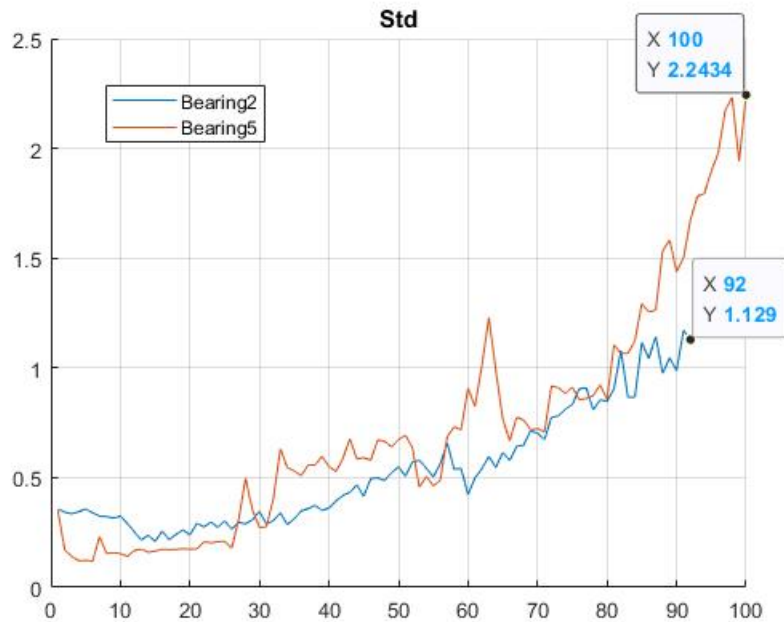


Figure 5.2: Plot of Standard Deviation for Bearing 2 vs. Bearing 5

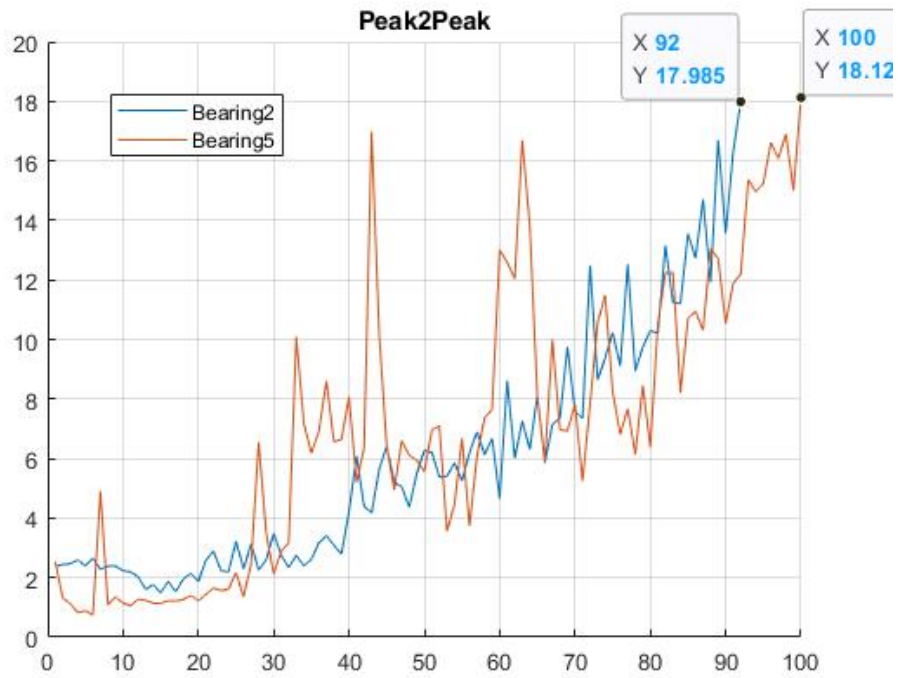


Figure 5.3: Plot of Peak to Peak for Bearing 2 vs. Bearing 5

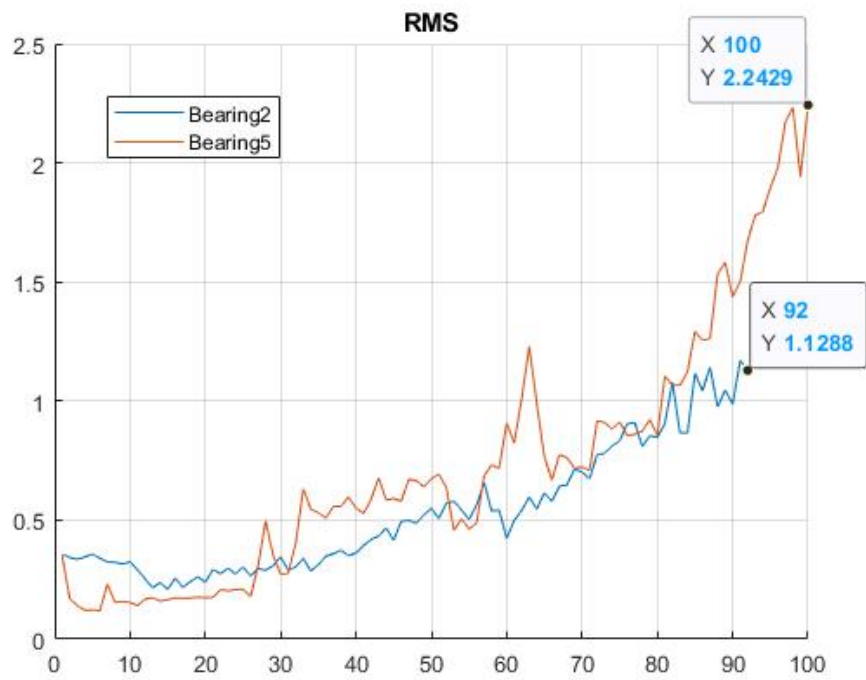


Figure 5.4: Plot of RMS for Bearing 2 vs. Bearing 5

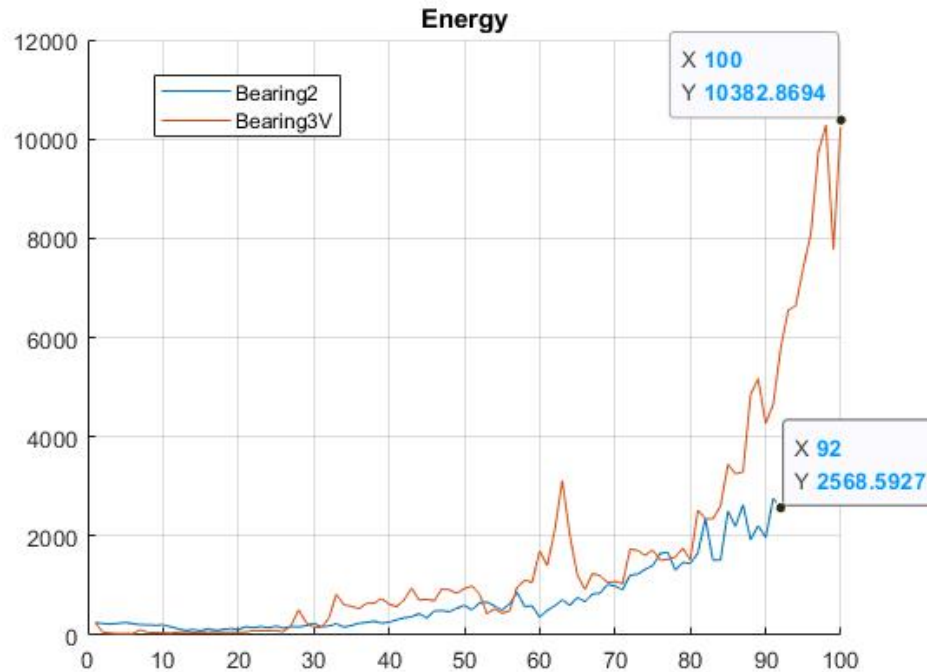


Figure 5.5: Plot of Energy for Bearing 2 vs. Bearing 5

The results are not good for our further research especially for the estimation of threshold. The final state for Peak to Peak is close to each other for these two experiments, but there are two peaks in the middle of plot for Bearing 5 which is abnormal. For other features, the wave is not so large as Peak to Peak feature, but there are big gap between the final state of tested bearings. Then the threshold for these bearings is very hard to estimate. More experiment shall be carried out to find out the distribution of threshold of these features.

### 5.1.2 Inverse Power Law Model

As discussed in Section 2.2.3, the relationship between the life time and stress level are inverse proportion. For Bearing 2 and Bearing 5,

- The life time for Bearing 2 is  $L_2 = 92 * 6 = 552$  mins;
- The life time for Bearing 5 is  $L_5 = 100 * 5 = 500$  mins;
- The stress for Bearing 2 is 3000 RPM and 2 spatter of mixture every 60 mins ( $f_{m2} = \frac{2}{60} = 0.0333$ );
- The stress for Bearing 5 is 3000 RPM and 1 spatter of mixture every 25 mins ( $f_{m5} = \frac{1}{25} = 0.04$ );

Therefore, according Equation 2.8, we have below calculation.

$$\begin{aligned}\frac{L_5}{L_2} &= \left(\frac{V_2}{V_5}\right)^n \\ \frac{L_5}{L_2} &= \left(\frac{f_{m2}}{f_{m5}}\right)^n \\ \frac{500}{552} &= \left(\frac{0.0333}{0.04}\right)^n \\ n &= 0.5397\end{aligned}\tag{5.4}$$

Then for stress of spatter frequency, we have Equation 5.5.

$$\frac{L_2}{L_1} = \left(\frac{f_{m1}}{f_{m2}}\right)^{0.5397}\tag{5.5}$$

This means the life time of bearings increases if the frequency of adding silicon carbide is reduced. The result shall be verified when there are more experiment results.

## 5.2 The First Passage Time

The calculation procedure has been well discussed, so only results are present in this section. As discussed in Section 5.1.1, four features are selected for calculation of the first passage time. Then the parameters for degradation shall be found out before the calculation.

### 5.2.1 Parameters Estimation through MLE

According to the equations mentioned in Section 2.2.4, parameters can be obtained through Equation 2.15 and 2.16 if the degradation follows wiener process. And parameters can be calculated through Equation 2.21 and 2.22 if it follows Geometric Brownian Motion. The results of calculation is shown as Table 5.4 and 5.5.

Feature	SDE	Bearing 2		Bearing 5	
		$\mu$	$\sigma$	$\mu$	$\sigma$
Standard deviation	Wiener Process	0.0018	0.0285	0.0032	0.0447
	GBM	0.0036	0.0468	0.0072	0.0886

Table 5.5: Result of Parameters (continue)

Feature	SDE	Bearing 2		Bearing 5	
		$\mu$	$\sigma$	$\mu$	$\sigma$
Peak to Peak	Wiener Process	0.0303	0.6816	0.0249	1.0945
	GBM	0.0091	0.1018	0.0249	0.3096
RMS	Wiener Process	0.0018	0.0285	0.0032	0.0477
	GBM	0.0036	0.0468	0.0072	0.0886
Energy	Wiener Process	5.4463	98.7659	15.0373	214.5585
	GBM	0.0095	0.0951	0.0225	0.2146

### 5.2.2 Inverse Gaussian Distribution

Previous chapter has discussed three methods to obtain the first passage time which are Inverse Gaussian distribution, numerical integration and Monte Carlo simulation. Since the results of these methods are similar with each other, Inverse Gaussian Distribution is selected to calculate the first passage time in this Section. The mean value and variance of the first passage time are calculated through Function 2.25 and 2.26 for wiener process and Function 2.28 and 2.29 for GBM. For the threshold, as shown in Table 5.3, none of the threshold is same with each other. The average termination value is used as the threshold of each feature. The results are listed in Table 5.6 and 5.7 for all four features which are Standard Deviation, Peak to Peak, RMS and Energy.

Table 5.6: Result of the First Passage Time

Feature	Values	Bearing 2		Bearing 5	
		Wiener Process	GBM	Wiener Process	GBM
Standard deviation	Mean	936.78	619.41	526.9375	480.71
	Variance	2.35E+05	2.16E+05	1.03E+05	3.52E+05
Peak to Peak	Mean	595.87	517.13	725.10	85.36
	Variance	3.02E+03	3.49E+05	1.40E+06	1.54E+04
RMS	Mean	936.58	619.43	526.83	480.71
	Variance	2.35E+05	2.16E+05	1.17E+05	3.52E+05

Table 5.7: Result of the First Passage Time (continue)

Feature	Values	Bearing 2		Bearing 5	
		Wiener Process	GBM	Wiener Process	GBM
Energy	Mean	1,189	650.38	430.64	112,700
	Variance	3.91E+05	2.37E+05	8.77E+04	1.87E+09

From the result of Table 5.6 and 5.7, all variance values are extremely high compared with the mean value. For the results in Chapter 4 with same method, the variance is less than 15% of the mean value. This shows the large uncertainty of the experiment's result. The uncertainty may be introduced by experiment directly or because of the small amount of samples used to get the parameters with MLE method. In addition, the large gap between the final state and average value also creates big uncertainty of the first passage time. Especially the final state of feature Energy, the terminate value of Bearing 5 is four times of Bearing 2 which amplified the variance. It is similar with feature Standard Deviation and RMS, the final value of Bearing 5 is around two times of Bearing 2. Before there is more understanding about these feature threshold, they are not good to estimate the first passage time.

In the other hand, the expected life time is compared with experiment results. The actual life time is 552 minutes for Bearing 2, and 500 minutes for Bearing 5. Compare the actual life time with the mean time of the first passage time in Table 5.6 and 5.7, the different is listed as Table 5.8.

Table 5.8: Difference between the Actual Failure Time and the Estimated Mean of the First Passage Time

Feature	Bearing 2		Bearing 5	
	Wiener Process	GBM	Wiener Process	GBM
Standard deviation	69.71%	12.21%	5.39%	-3.86%
Peak to Peak	7.95%	-6.32%	45.02%	-82.93%
RMS	69.67%	12.22%	5.37%	-3.86%
Energy	115.40%	17.82%	-13.87%	22440%

For Bearing 2, the performance of GBM is better than wiener process especially for feature Standard deviation, RMS and Energy. It means GBM is more suitable to be selected as SDE to analysis the degradation of Bearing 2. This fits the understand of the physical mechanisms

which the degradation is related to both time and current values. While for Bearing 5, the situation is different. The expected first passage time calculated by Peak to Peak and Energy is much higher than the experiment result. They cannot be used as feature to predict the first passage time. Considering all the result, it is clear that feature Standard Deviation and RMS is better on the first passage time prediction, especially when they use GBM model. This is in accordance with the result of feature importance in Table 5.2.

The difference between the mean first passage time and the true value might be caused by following reasons.

- Uncertainty of original data may lead the wrong result of calculation.
- The small amount of samples used to get the parameters with MLE method.
- The setting of the threshold is estimated with only two groups of data. More experiments shall be carried to find out the distribution of threshold.
- The method used for calculation has higher variance than other methods. Numerical integration shall be used for calculation.

### 5.3 Digital Twin Models

The Predictive Maintenance Toolbox of Matlab is used for the digital twin model. It is an exponential degradation model for predicting the Remaining Useful Life (RUL). The model is able to detect the significant degradation trend in real time and updates its parameter priors when a new observation becomes available. The example follows a typical prognosis workflow: data import and exploration, feature extraction and post processing, feature importance ranking and fusion, model fitting and prediction, and performance analysis. Data from Bearing 5 is used in the digital twin model of this section. Detail process is discussed and present as following sections.

#### 5.3.1 Feature Extraction and Post-processing

The functions of features have been present in Table 5.1. Since there are noise associated with the extracted features, and the noise can be harmful to the RUL prediction. A moving mean filter is applied to the extracted features. Then the moving mean smooths the feature values and help to make result more reliable. Figure 5.6 plots the value of RMS feature of Bearing 5 before and after smoothing. It is clear that the value after smoothing is less noise with same trend.



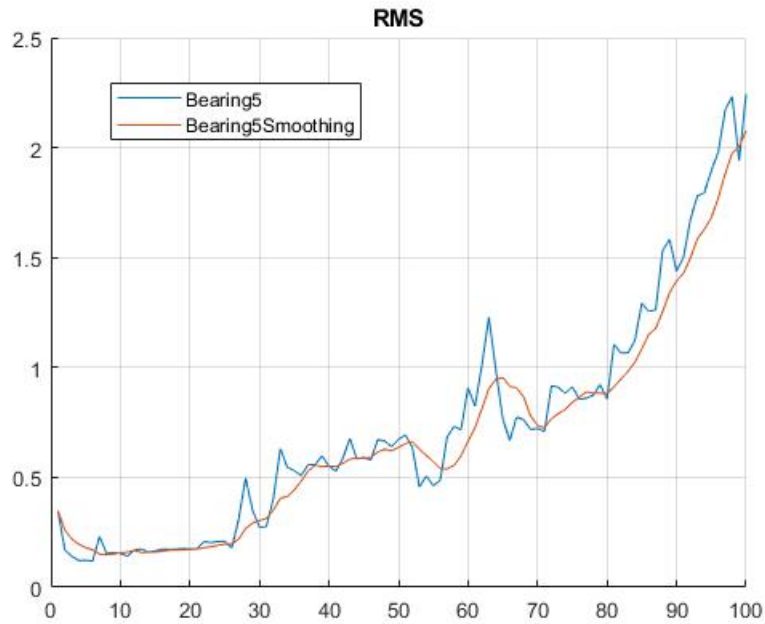


Figure 5.6: Plot of RMS Feature of Bearing 5 before and after Smoothing

### 5.3.2 Feature Importance Ranking and Fusion

After data smoothing, parts of data shall be trained to select features used in digital twin model. Normally, the data collected in the early stage is used to find the property of system. In this section, the first 40 examples data are used for training. And the feature importance ranking is based on the trained data. Function 5.2 is used to calculate the monotonicity of all features, the result is shown as Figure 5.7. Features with feature importance score larger than 0.3 are selected for feature fusion in the next section. The selected features are Standard deviation, RMS, Energy and Peak to Peak.

Principal Component Analysis is used to fuse the selected features. As discussed in Section 2.2.5, it is very common to use PCA as dimension reduction and feature fusion method. The model uses the selected trained data to get the PCA coefficients, the mean and the standard deviation used in normalization. These values are used for the entire model. Plot the value of these principal components. Figure 5.8 shows the result. The plot shows that the PCA1 and PCA3 are increased together with the degradation while PCA2 is reduced with the degradation. Since it is obviously that the percentage of PCA2 is a small part in total. So PCA1 shall be chosen as the health indicator. Visualize the health indicator, the plot is shown as Figure 5.9.

The health indicator plot goes a bit down and remains constant in the beginning from start point until sample 30, and then waves in the middle part from sample 30 to sample 80. The

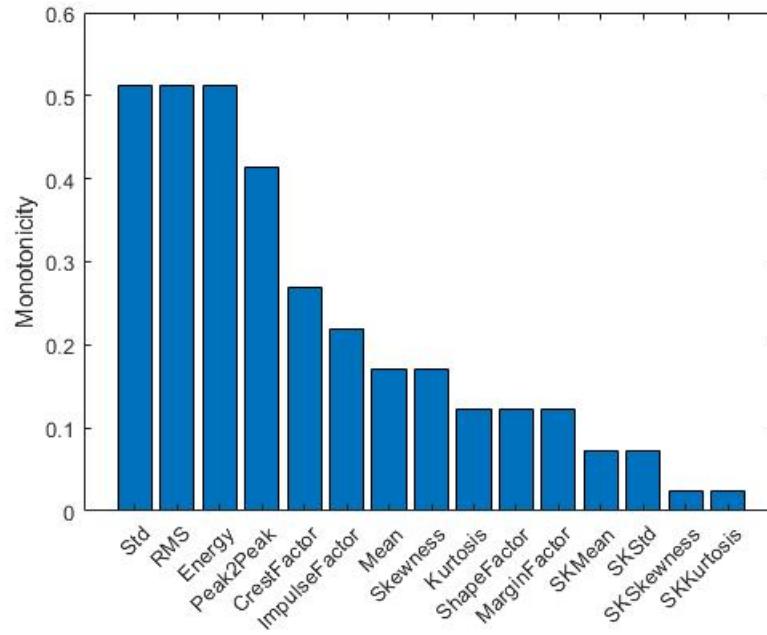


Figure 5.7: Monotonicity value of all features for Bearing 5

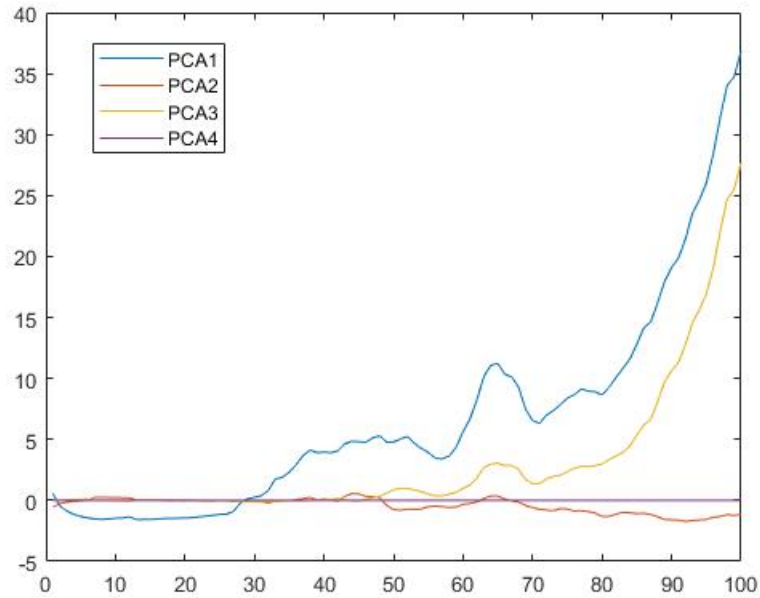


Figure 5.8: Plot of Principal Component 1<sup>st</sup>, 2<sup>nd</sup>, 3<sup>rd</sup>, 4<sup>th</sup>

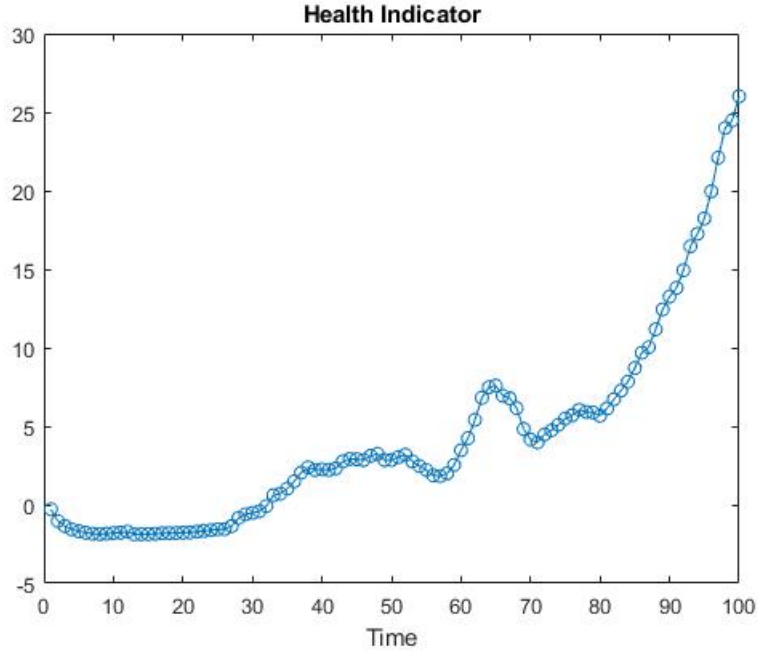


Figure 5.9: Plot of Health Indicator of Bearing 5

footprint of waves becomes shorter, and wave height becomes larger. From sample 80, it grows deeply until failure occurs.

### 5.3.3 Model Fitting and Prediction

The model used for RUL estimation is exponential degradation model which can be defined as Equation 5.6

$$h(t) = \phi + \theta \cdot \exp\left(\beta t + \varepsilon - \frac{\sigma^2}{2}\right) \quad (5.6)$$

where  $h(t)$  is the health indicator as function of time.  $\phi$  is a constant.  $\theta$  and  $\beta$  are random parameters determined the slope of the model, where  $\theta$  is log-normal distributed and  $\beta$  is Gaussian distributed. And at each time  $t$ , the distribution of  $\theta$  and  $\beta$  is updated based on the latest  $h(t)$ .  $\varepsilon$  is a Gaussian white noise following normal distribution with parameters  $N(0, \sigma^2)$ . The  $-\frac{\sigma^2}{2}$  in the exponential is to make the expectation of  $h(t)$  satisfy Equation 5.7

$$E[h(t) | \theta, \beta] = \phi + \theta \exp(\beta t) \quad (5.7)$$

The threshold of the model shall be selected according to the historical data or experience. Since there is no historical data, it uses the last value of health indicator. The variance of the slope parameters are set very large, so the model is mostly relying on the observed data. Param-

eters are given as Table 5.9.

Table 5.9: Value of Parameters

Parameter	Value
$mean(\theta)$	1
$Var(\theta)$	$10^6$
$mean(\beta)$	1
$Var(\beta)$	$10^6$
$\phi$	-1
$Var(\varepsilon)$	$\left(\frac{0.1 * threshold}{threshold - \phi}\right)^2$
Slope detection level	0.1

Then use Matlab toolbox "predictRUL" to predict the RUL and update the parameter in real time. The result for the lastest sample is shown as Figure 5.10.

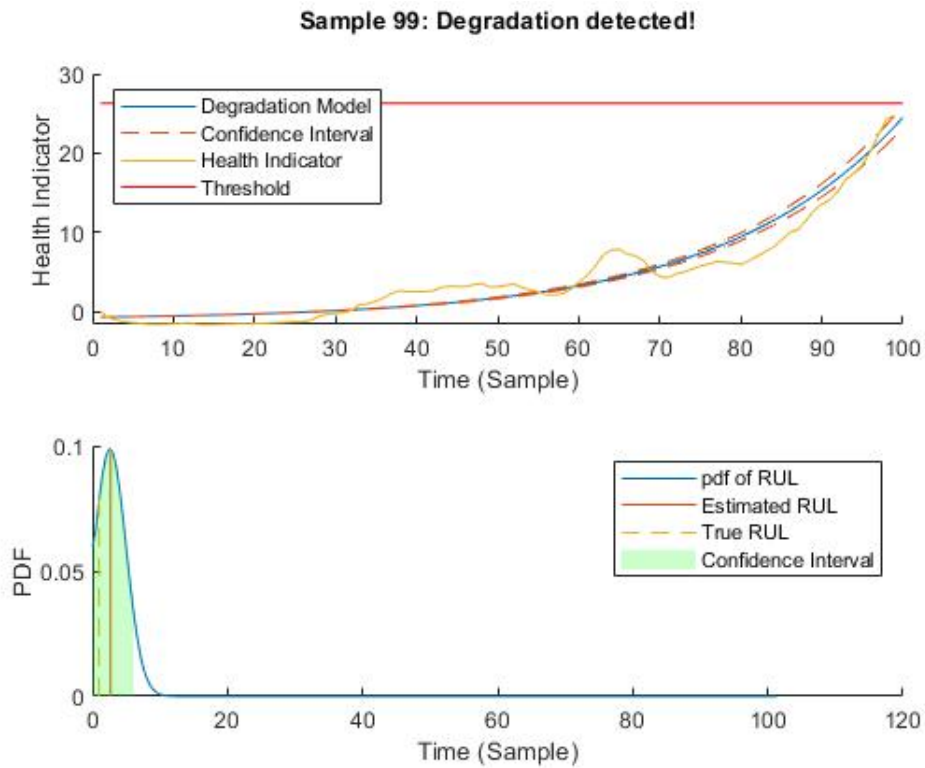


Figure 5.10: Model Result of Sample 99

The example also provides an animation of the real-time RUL estimation which shown the degradation model every sample. It gives expression of the RUL changing due to the new data collected. Plot of date 1, 10, 20, 30, 40, 50, 60, 70, 80, 90 and 99 are shown in Appendix C. From those plots, it's clear that the lines of degradation model, confidence interval and health indicator are changed when the model running. And the bearing is closed to failure on the last sample.

### 5.3.4 Performance Analysis

Saxena et al. (2010) proposes a method of prognostic performance analysis which is  $\alpha - \lambda$  plot. The method calculates the probability that the estimated RUL is between the  $\alpha$  bound and the true RUL. And then it uses the probability as a performance metric of the model. The  $\alpha$  bound is set as 20%.

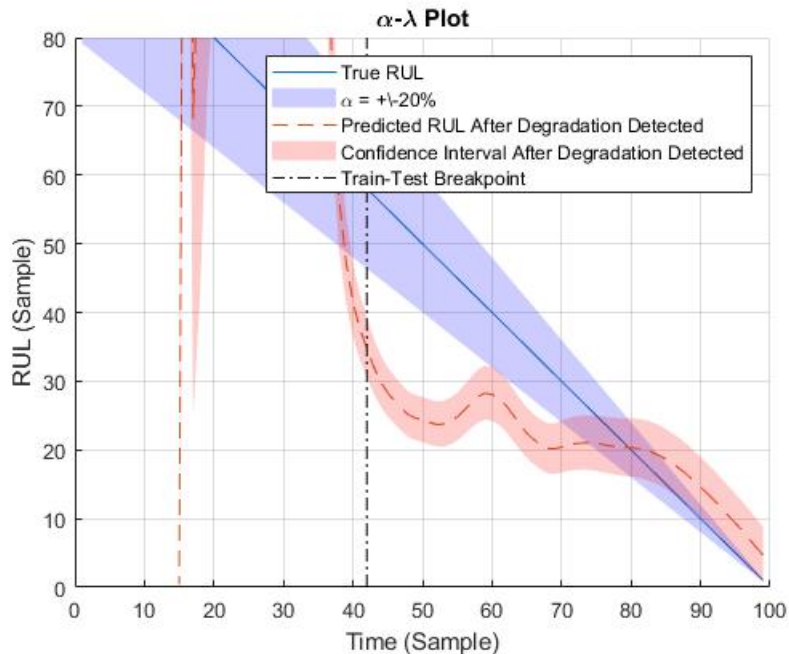


Figure 5.11:  $\alpha - \lambda$  plot

Figure 5.11 is  $\alpha - \lambda$  plot for Bearing 5. Findings are as below:

1. The predicted RUL does not have same trend with the true RUL for training data.
2. Before sample 80, the predicted RUL is lower than the true RUL with one wave around sample 60.
3. After sample 80, the predicted RUL is higher than the true RUL.

4. The confidence interval is closed to the  $\alpha$  bound after sample 80.
5. The predicted life time is less than 4% higher than the true life time after sample 70.
6. Even the predicted RUL is far from the true for the training data period and the beginning of prediction, the model brings the predicted RUL back to the true value in the end of calculation. This shows the ability of self-correction of digital twin model.
7. The performance of model is better when there are more data input.

# Chapter 6

## Discussion

### 6.1 Experiment Design

The experiment did not complete original plan for the second stage due to the delay of logistics of bearings and lab control caused by COVID-19. In the end of the semester, only two groups of data set can be used for analysis.

The results of preprocessing data do not fit the expectation well. From Table 5.2, the result of feature importance are low for most of the features and varies for different data set. For example, feature Kurtosis is a popular used feature for prediction of bearings' status, such as [Tian et al. \(2015\)](#). While the feature importance is very low for all bearing's results. It means the Kurtosis feature from the experiment is not consistent with the degradation. Other features have to be considered.

The results of Inverse Power Law Model is shown as Equation 5.5. It can be used to find out the relationship between the stress level and life time. More experiments results shall be used to verify the conclusion.

The results of experiment is not constant. The uncertainty of the experiment might caused by following reasons. Possible solutions are proposed accordingly.

- Unstable time interval caused by saving data manually. The system is planned to upgrade in July to save data automatically. The time interval could keep constant then.
- The stress of contaminated lube oil is added manually. In the other hand, the silicon carbide might be thrown out of the bearing during high speed rotation. Therefore, it is hard to control the amount of silicon carbide inside bearing and the frequency of increasing stress level. Since the space inside bearing is limited, the amount of silicon carbide shall

not add too much for one time. In addition, the frequency of adding silicon carbide shall be low to keep bearing operating under stable stress. However, this will extend the life time of bearings and cost longer time for testing.

- From the plots of features, there are a higher wave around sample 60 for all features of both bearings compared with other period. It might caused by one systematic reason which shall be investigated further.
- The value of acceleration data is used as termination condition of the experiment. It may not correspond with the threshold of extracted features. More experiment shall be carried out to find out the relationship between the features' threshold and acceleration data.
- Uncertainty might caused by multiple operators. Clearly experiment procedure shall be prepared in document and followed strictly to avoid wrong operation. Form for experiment log is proposed as Appendix B.
- Experiment data shall be analysed once the testing completed to avoid repeating simple errors.

## 6.2 Maintenance Models

### 6.2.1 The First Passage Time Models

There are three models introduced for the first passage time. The results with assumed parameters have been present and discussed in Chapter 4. The summary of findings are as below

- Inverse Gaussian distribution is the most rough methods which has the highest variance value. In the same time, the result is constant when parameters are fixed and it is the easiest method to be implemented.
- Integration methods has the least variance and the process could help us to understand the distribution while degradation. However, it is much more complex than the others.
- The expected value  $E(T)$  from Monto Carlo simulation is uncertain every time since the process is simulated randomly. Therefore, the result is not very reliable. To get a better result, the number of loop shall be as large as possible.
- There are two definitions for GBM, then the results are slightly different when definition of GBM is changed. Log-normal distribution definition can be implemented on all three methods. But normal distribution definition cannot be used in Inverse Gaussian distribution method. The results are different if different definition of GBM is used but similar



when definition is same. This means the affects from definition is larger than the affects caused by the methods. The mean value used log-normal distribution is always smaller than normal distribution which means the degradation process is faster when it is log-normal distributed.

- All the calculation is based on the assumption of fixed threshold. If the threshold is varying, it does not follow the Inverse Gaussian distribution. Numerical integration method shall be used by times distribution of the threshold with the PDF of first passage time and integrate the product.

When the experiment data is implemented with Inverse Gaussian distribution of the first passage time, the variance of the first passage time is extremely high compared with the theoretical calculation. The results are shown in Table 5.6 and 5.7. The high variance might be caused by following reasons.

- Uncertainty introduced by experiment directly .
- The small amount of samples used to get the parameters with MLE method.
- The setting of the threshold is estimated with only two groups of data. More experiments shall be carried to find out the distribution of threshold.
- The method used for calculation has higher variance than other methods. Numerical integration shall be used for calculation.

The difference between the actual failure time and the estimated mean of the first passage time is present in Table 5.8. The situation is different for Bearing 2 and Bearing 5. The data set of Bearing 2 is more suitable to used GBM as SDE for analysis. While for Bearing 5, feature Peak to Peak and Energy are 83% and 22440% difference with the true value. They cannot be used to predict the remaining useful life. Generally speaking, the GBM model for feature Standard deviation and RMS is good choice to calculate the first passage time.

### 6.2.2 Digital Twin Model

Digital twin model is implemented with experiment data. The finding of results is listed as below

- The predicted RUL does not have same trend with the true RUL for training data period.
- Before sample 80, the predicted RUL is lower than the true RUL with one wave around sample 60.
- After sample 80, the predicted RUL is higher than the true RUL.

- The confidence interval is closed to the  $\alpha$  bound after sample 70 until the end.
- The predicted life time is less than 4% higher than the true life time after sample 70.
- Even the predicted RUL is far from the true for the training data period and the beginning of prediction, the model brings the predicted RUL back to the true value in the end of calculation. This shows the ability of self-correction of digital twin model.
- The performance of model is better when there are more data input.

### 6.2.3 Comparison between Models

The models chosen to compare are Inverse Gaussian distribution model for the first passage time and digital twin model for RUL prediction. The two models have different perspective, principle and procedure. The data set used on both models are experiment results of Bearing 5. However, the final result for expected life time is adjacent to each other. The best result of expected first passage time is 3.86% shorter than the true value by the first passage time model. While the predicted life time is less than 4% higher than the true value according to the prediction of digital twin model after sample 80. The comparison between these models are listed as below.

- The model for first passage time deals with features one by one. The feature which has the highest importance is chosen to predict the first passage time.
- The digital twin model uses several features' fusion to predict the RUL which reduce the probability of misleading by one feature.
- For Bearing 5, the RMS smoothing plot 5.6 is similar with the health indicator plot 5.9. It means that they are equivalent in the example.
- The digital twin model used parts of data for ranking and selecting data. If the stress level changed during later process, the result will be wrong.
- There are several SDE to be used as foundation of the first passage time model. The selection of SDE shall be based on the large amount of experiments result analysis.
- The parameters estimation of the first passage time needs a large amount of data set to enhance the quality of estimation. Time interval between samples shall be set shorter.
- The digital twin model mainly based on the latest value of health indicator and may improve the prediction if the stress keep constant.

- Both models requires good knowledge about the threshold of bearings. More experiments shall be done to get enough information.
- Three methods for the first passage time provide more choices for the prediction tools.
- The results from digital twin is far from true value in the middle of prediction period. While the accuracy of the first passage time is more guaranteed.
- Numerical integration method for the first passage time could help to understand the degradation process.
- Both models have been verified with theoretical data and experiment data.
- Both models could be implemented to other components of wind turbines.

# Chapter 7

## Conclusions and Recommendations for Further Work

### 7.1 Conclusions

For offshore wind turbine, maintenance plan for minor failures shall be pay more attention than for onshore projects. Therefore, the master thesis investigates several maintenance models and compares the results to find suitable models for improving the maintenance of wind turbines. The conclusions are as following:

Firstly, the experiments of bearing degradation are run in RAMS lab for obtaining real degradation for models testing. Although there is still some problems about the experiment setting and data uncertainty, it provides a good opportunity to understand the degradation mechanism and chance to practise maintenance models with real data. Some advice are given for improving the experiments in future.

Secondly, Features are extracted from the observations of experiment and selected by the value of monotonicity.

Thirdly, three methods for CDF of the first passage time are investigated and implemented. The selected stochastic differential equations are wiener process and Geometric Brownian motion. The results with assumed parameters are present and compared. All methods have some advantage and disadvantage and could be selected to use as needed.

Fourthly, the first passage time model is compared with digital twin model with the experiment data. The final results are consistent with each other. The benefit of digital twin is self correction during the predict process especially in the later stage. All these models could be

used to improve maintenance strategy later.

## 7.2 Discussion

For the first passage time model, the thesis only considered models which have a fixed and known failure threshold, it is obvious relevant to find the first hitting time. However, the failure threshold is not always constant, or at least not known. This means that the threshold shall be formulated as a random quantity. The calculation is not included with the thesis but it is possible to integrate over the uncertainty distribution. Then the first passage time would not be Inverse Gaussian distributed. A model where a fixed failure threshold could be reasonable is fatigue cracks developing to a breakage at a given crack length. For an ideal piece of material this could be reasonable, but for a complex geometry it would be impossible to find the critical crack length as a deterministic quantity.

Furthermore, the “first” passage time is not always the most relevant for component failure, for example it could be the “second” hitting time, or another measure where a failure occurs when it has been in the risk zone for some time. In particular for health indicators that are derived, there is no guarantee that such a failure threshold exist. More research shall be done when there is more information about the threshold distributions.

## 7.3 Recommendations for Further Work

Due to the limitation of computer skills, available data and time of project, there are still a lot of jobs to do within the scope of the project. It is recommended to take following work for further researches.

- More experiments shall be carried out to have more understanding of the threshold the features.
- Use numerical integration methods to find out the first passage time with variable threshold.
- Feature fusion methods could be implemented in the first passage time models to have better results.
- The function in digital twin model could be replaced by wiener process or Geometric Brownian motion. It is possible to improve the result of prediction.

- Skills of data processing shall be practising for modeling in future.
- The methods mentioned in [2.2.2](#) can be used to obtain degradation parameters if data could be saved automatically.
- Create Digital Twin model for maintenance of more components of wind turbine or wind farm.

# Appendix A

## Acronyms

**ALT** Accelerated Life Testing

**CDF** Cumulative Distribution Function

**ISO** the International Organization for Standardization

**MLE** Maximum Likelihood Estimation

**ms** Millisecond

**MTTF** Mean time to failure

**PALT** Progressive-stress Accelerated Tests

**PCA** Principal Component Analysis

**PDF** Probability Density Function

**RAMS** Reliability, Availability, Maintainability, and Safety

**RMS** Root Mean Square

**RPM** Revolutions Per Minute

**RUL** Remaining Useful Life

**SALT** Step-stress Accelerated Tests

**SDE** Stochastic Differential Equation

**SK** Spectral Kurtosis

**Std** Standard deviation

# Appendix B

## Form for Experiment Record

Here shows the proposed form for experiment record and the record for the 5<sup>th</sup> bearing as an example.



## Experiment form

---

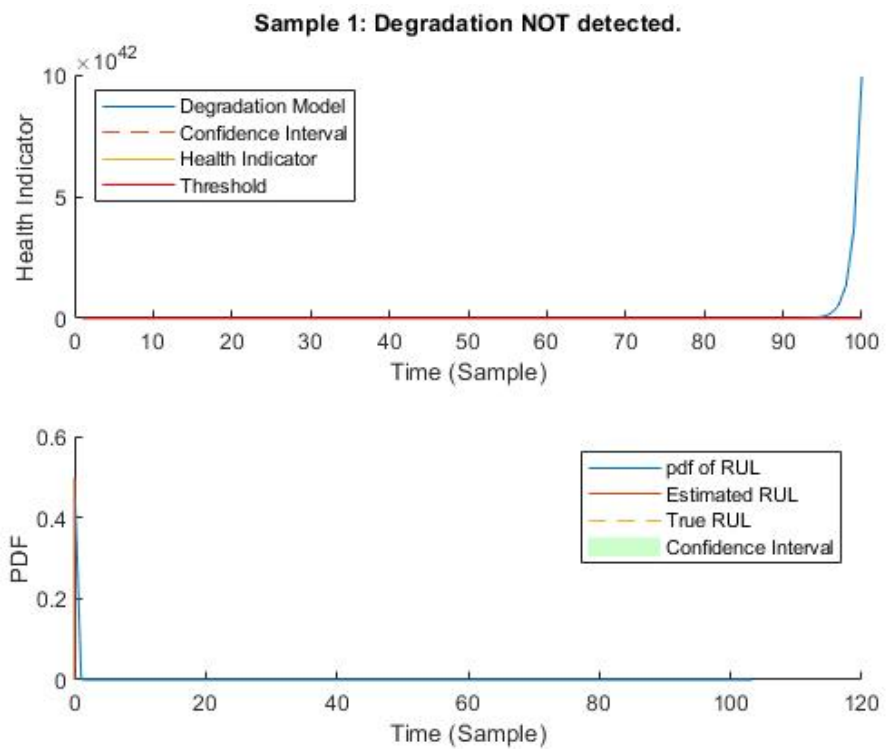
Bearing No.					Date		
Activity	Start time	End time	Reason				
1							
2							
3							
4							
Data time interval							
Stress level (Target stress shall be marked)							
Speed			Size of silicon			Density of silicon	
rpm			S	M	L	%	
Stress change log							
	Start time	End time	Note		Start time	End time	Note
1				7			
2				8			
3				9			
4				10			
5				11			
6				12			
Summary							
Highest accelerate value			g	Lowest accelerate value		g	
Note							
Number of data file					Prepared by		

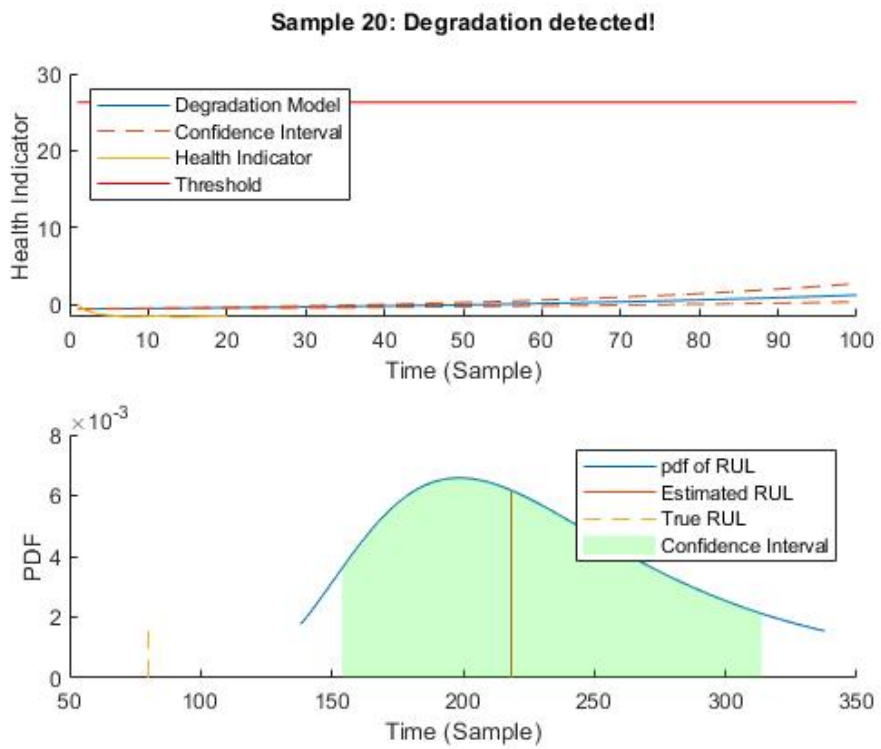
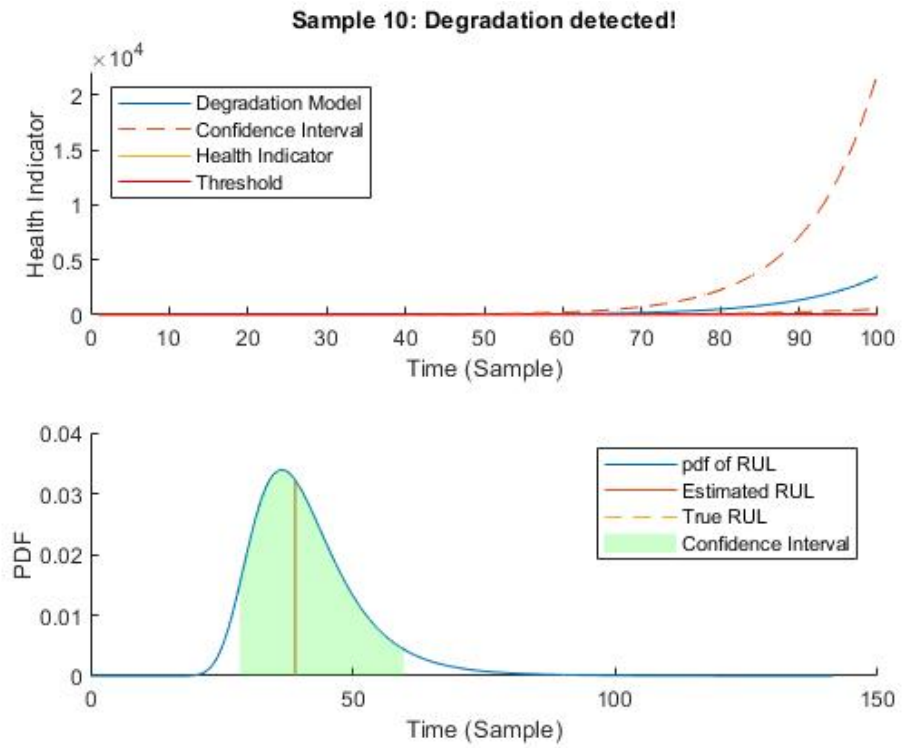
## Experiment form

Bearing No.	5				Date	2020-05-22					
Activity	Start time	End time	Reason								
1	8:48	10:08	Compute required to restart.								
2	10:13	18:06	No stress between data 16 and 16-1, saved for comparing between stops.								
3											
4											
Data time interval			5mins								
Stress level (Target stress shall be marked)											
Speed				Size of silicon				Density of silicon			
3005rpm(input), 2975rpm(system)				S	M	L	1 pour /time, 0.72 grams				
Stress change log											
	Time		Time		Time		Time		Time		Time
1	8:53	7	11:28	13	13:58	19	16:28				
2	9:18	8	11:53	14	14:23	20	16:53				
3	9:43	9	12:18	15	14:48	21	17:18				
4	10:13	10	12:43	16	15:13	22	17:43				
5	10:38	11	13:08	17	15:38	23					
6	11:03	12	13:33	18	16:03	24					
Summary											
Highest accelerate value			9.711 g (110b)				Lowest accelerate value			-10.162 g (110b)	
Note	Train IB ACC IBY ia.csv Tested bearing, Vertical data				Train IB ACC IBX ib.csv Tested bearing, Horizontal data						
	Train OB ACC OBY ic.csv Balance bearing, Vertical data				Train OB ACC OBX id.csv Balance bearing, Horizontal data						
	No mixture left. To be changed next time.										
Number of data file			110*4				Prepared by			Jie Liu	

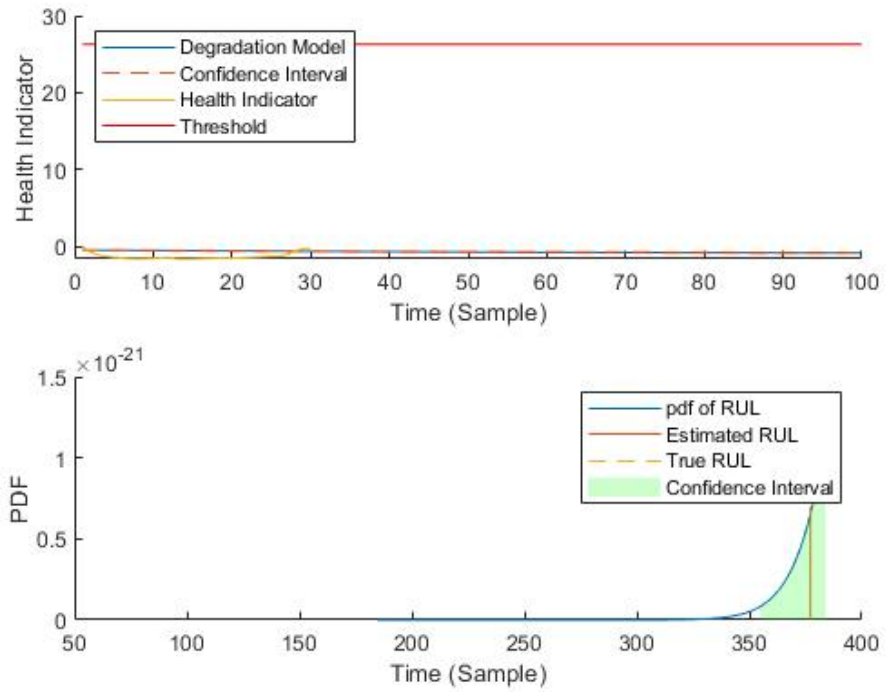
# Appendix C

## Plot of RUL Result of Digital Twin with Experiment Data

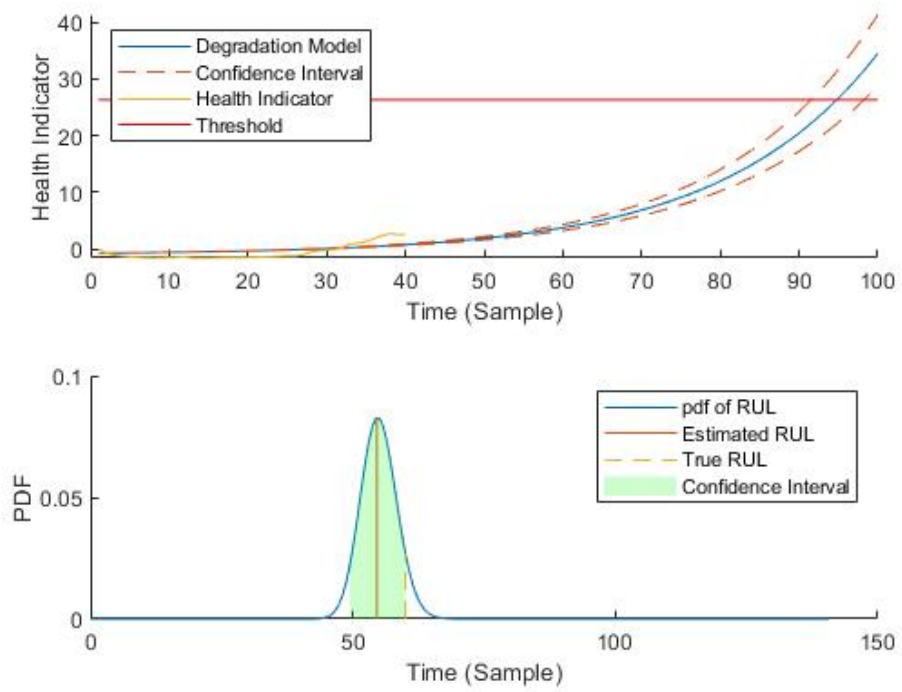




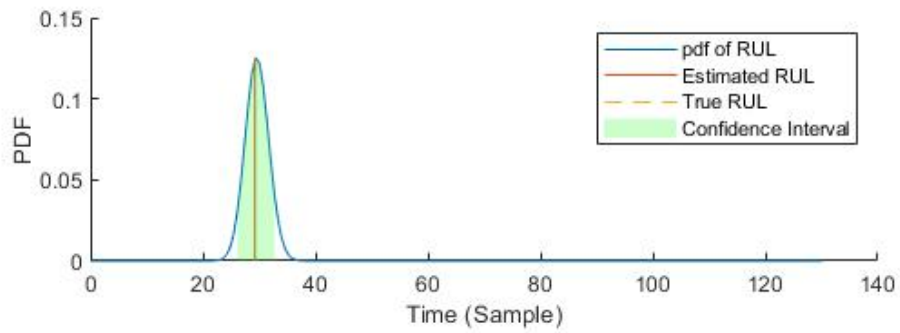
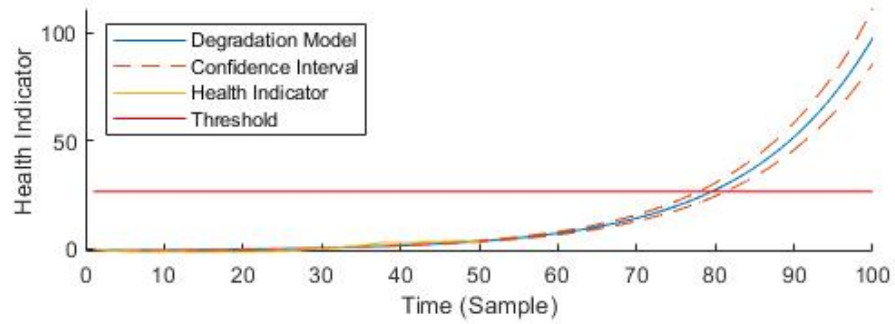
**Sample 30: Degradation detected!**



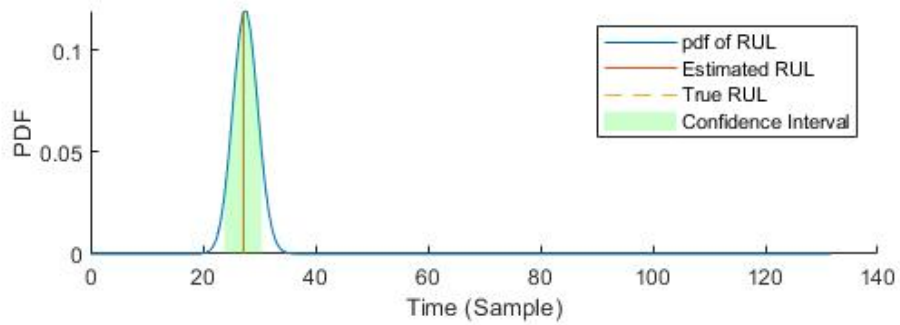
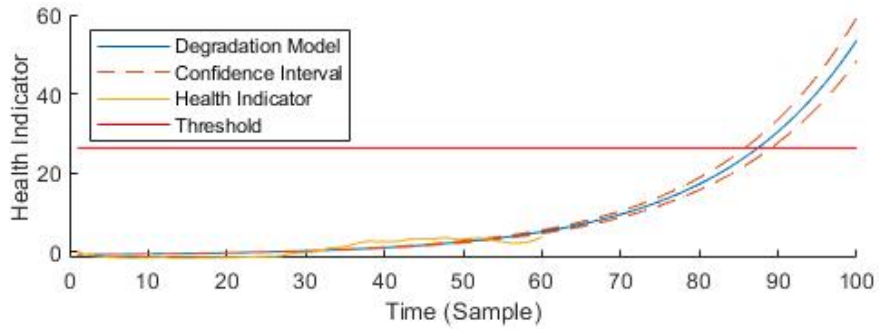
**Sample 40: Degradation detected!**



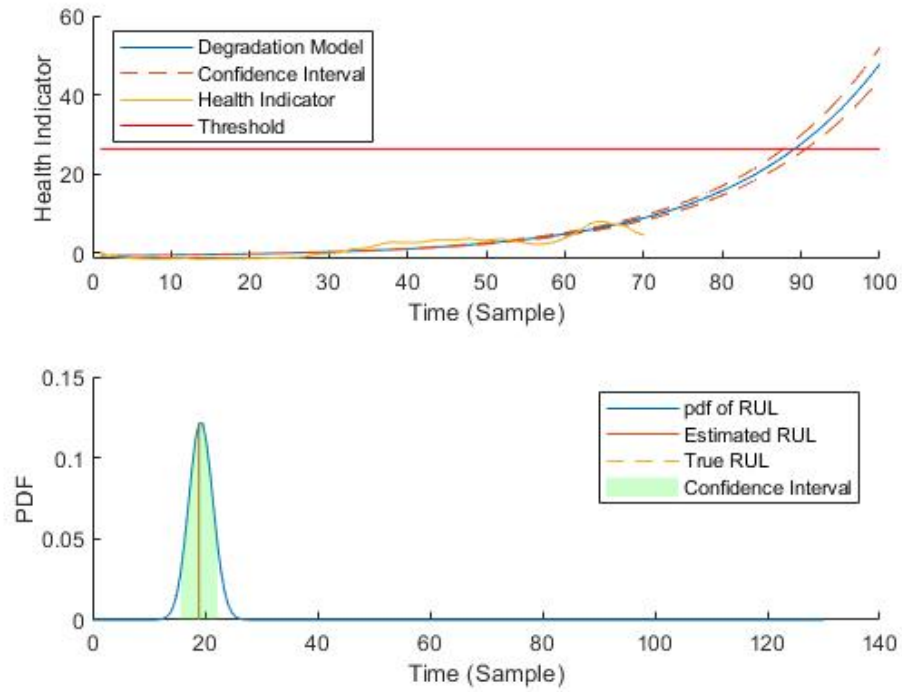
**Sample 50: Degradation detected!**



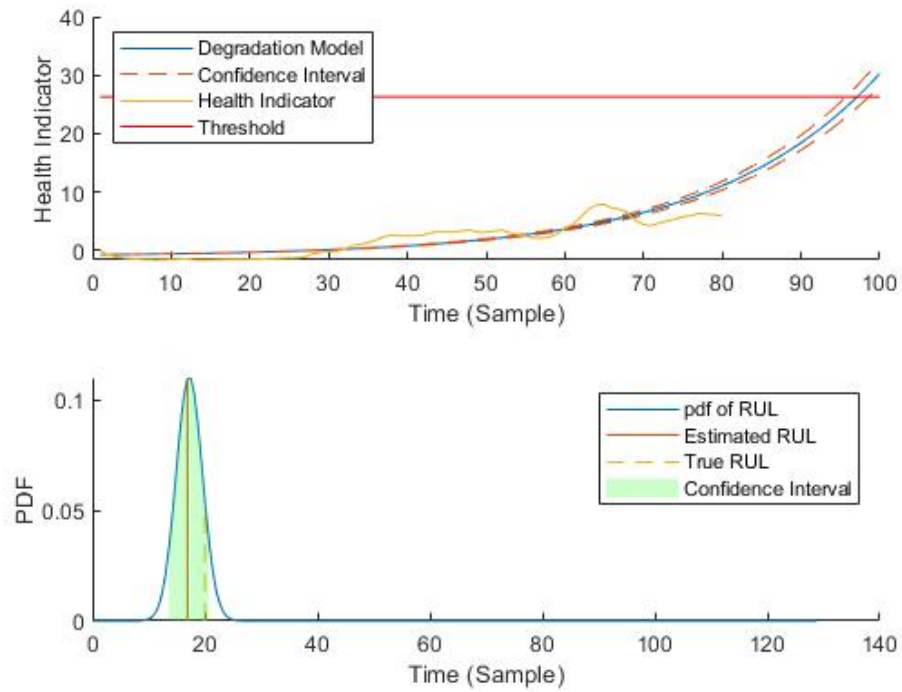
**Sample 60: Degradation detected!**



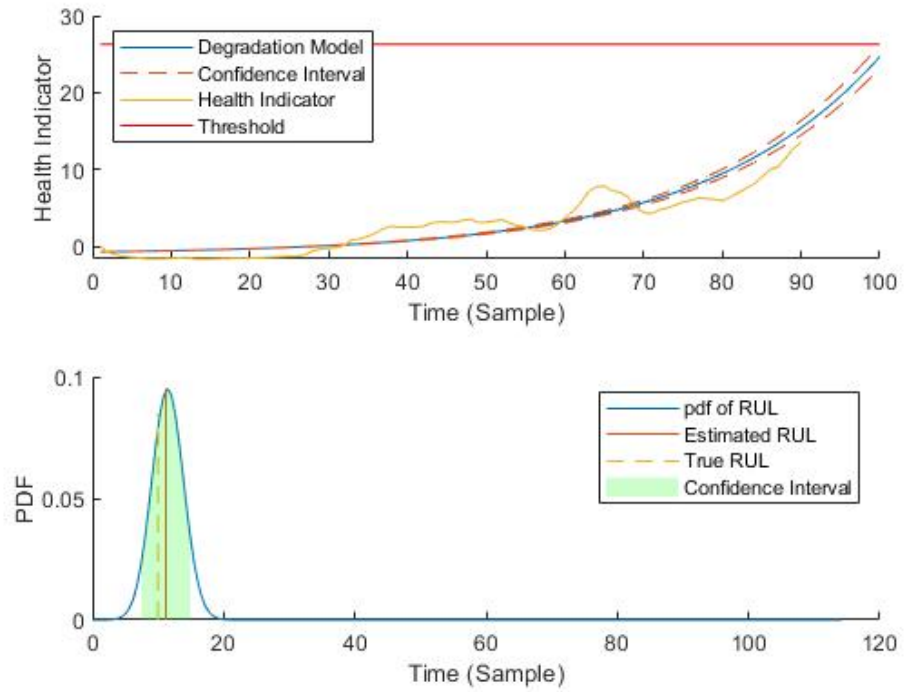
**Sample 70: Degradation detected!**



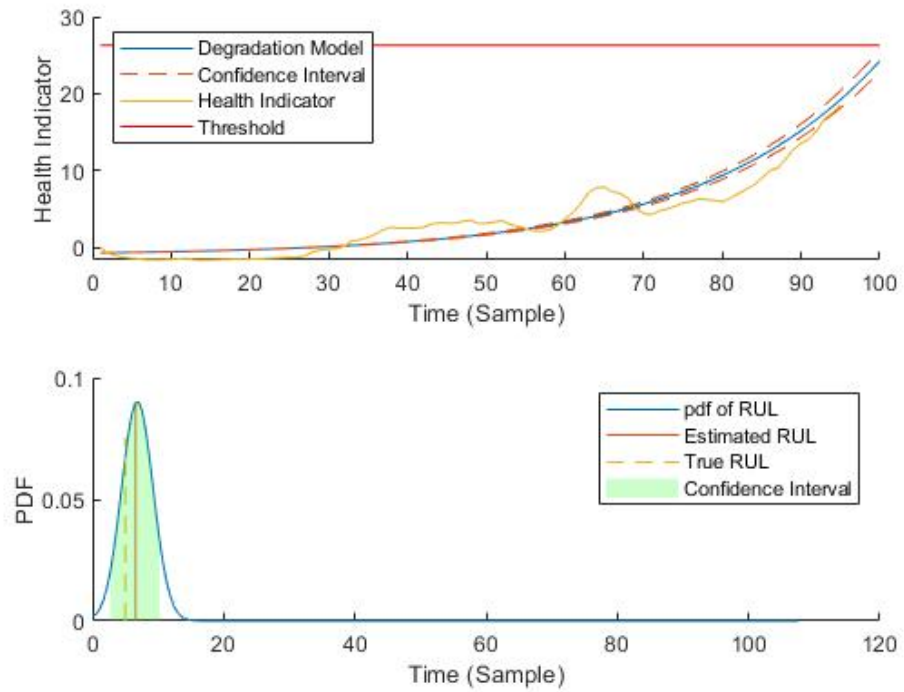
**Sample 80: Degradation detected!**



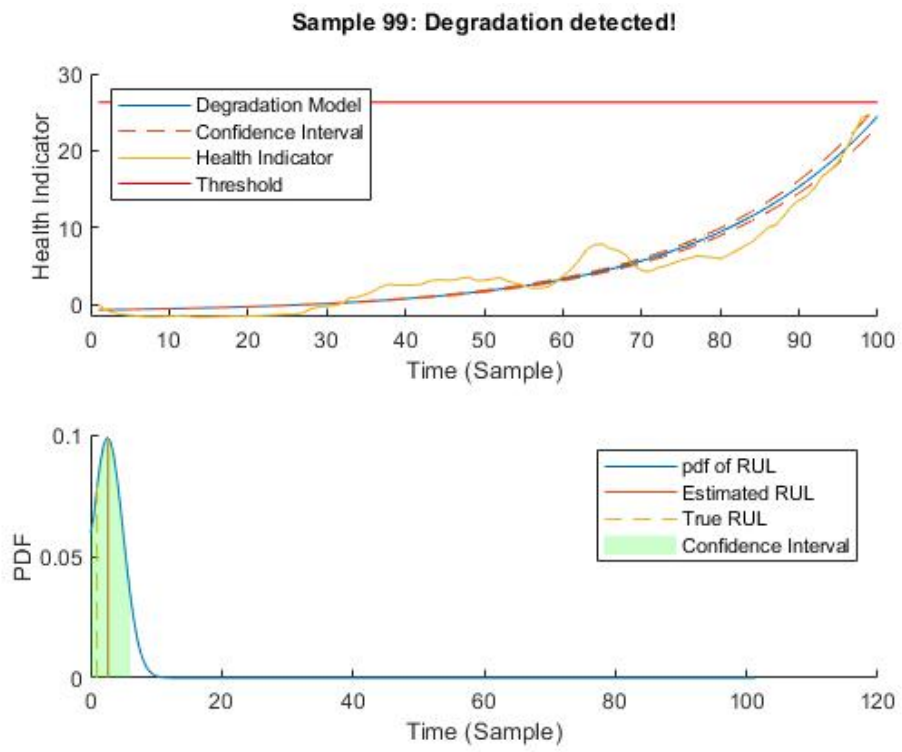
**Sample 90: Degradation detected!**



**Sample 95: Degradation detected!**







# References

- Abundo, M. (2010). First-passage problems for one-dimensional diffusions with random jumps from a boundary. *Stochastic Analysis and Applications*, 29(1), 121–145.
- Ali, J. B., Saidi, L., Harrath, S., Bechhoefer, E., & Benbouzid, M. (2018). Online automatic diagnosis of wind turbine bearings progressive degradations under real experimental conditions based on unsupervised machine learning. *Applied Acoustics*, 132, 167–181.
- Barros, A. (2019). Tpk4450 data driven prognostic and predictive maintenance. *Course memo*, 22–43.
- Bechhoefer Eric, D. H., Brandon Van Hecke. (Oct. 2013). Processing for improved spectral analysis. In *Annual conference of the prognostics and health management society*. New Orleans, LA,. Retrieved from <http://data-acoustics.com/measurements/bearing-faults/bearing-3/>
- Bently, D. (2020, May). *Donald bently | college of engineering | the university of iowa*. [www.engineering.uiowa.edu](http://www.engineering.uiowa.edu).
- Blasi, R., Nakazato, H., Namiki, M., & Pascazio, S. (1997). Emergence of a wiener process as a result of the quantum mechanical interaction with a macroscopic medium. *Physica A: Statistical Mechanics and its Applications*, 245(1-2), 189–211.
- Caroni, C. (2017). *First hitting time regression models: Lifetime data analysis based on underlying stochastic processes*. John Wiley & Sons.
- Chambers, R. L., Steel, D. G., Wang, S., & Welsh, A. (2012). *Maximum likelihood estimation for sample surveys*. CRC Press.
- Cheridito, P. (2001). *Regularizing fractional brownian motion with a view towards stock price modelling* (Unpublished doctoral dissertation). ETH Zurich.
- Coble, J. B. (2010). Merging data sources to predict remaining useful life—an automated method to identify prognostic parameters.

- Dennis, B., Munholland, P. L., & Scott, J. M. (1991). Estimation of growth and extinction parameters for endangered species. *Ecological monographs*, 61(2), 115–143.
- Erikstad, S. O. (2017). Merging physics, big data analytics and simulation for the next-generation digital twins. *High-Performance Marine Vehicles*, 141–151.
- Faulstich, S., Hahn, B., & Tavner, P. J. (2011). Wind turbine downtime and its importance for offshore deployment. *Wind energy*, 14(3), 327–337.
- Fisher, R. A. (1936). Design of experiments. *Br Med J*, 1(3923), 554–554.
- Fisher, R. A. (1992). Statistical methods for research workers. In *Breakthroughs in statistics* (pp. 66–70). Springer.
- Galván-Núñez, S., & Attoh-Okine, N. (2018). A threshold-regression model for track geometry degradation. *Proceedings of the Institution of Mechanical Engineers, Part F: Journal of Rail and Rapid Transit*, 232(10), 2456–2465.
- Gitelman, L., Kozhevnikov, M., & Kaplin, D. (2019). Asset management in grid companies using integrated diagnostic devices. *International Journal of Energy Production and Management*, 4(3), 230–243.
- Glaessgen, E., & Stargel, D. (2012). The digital twin paradigm for future nasa and us air force vehicles. In *53rd aiaa/asme/asce/ahs/lasc structures, structural dynamics and materials conference 20th aiaa/asme/ahs adaptive structures conference 14th aiaa* (p. 1818).
- GOST, R. (n.d.). 55265.7-2012 (iso 10816-7: 2009) vibration. *Monitoring the state of machines by measuring vibration on non-rotating parts. Part, 7*.
- Grieves, M. (2014). Digital twin: Manufacturing excellence through virtual factory replication. *White paper*, 1–7.
- Hendry, D. F., & Nielsen, B. (2007). *Econometric modeling: a likelihood approach*. Princeton University Press.
- Hu, Y., Li, H., Shi, P., Chai, Z., Wang, K., Xie, X., & Chen, Z. (2018). A prediction method for the real-time remaining useful life of wind turbine bearings based on the wiener process. *Renewable energy*, 127, 452–460.
- Itô, K. (1944). 109. stochastic integral. *Proceedings of the Imperial Academy*, 20(8), 519–524.
- Jing-Yuan, Z., Wei-Gang, S., & Guan-Rong, C. (2012). Exact scaling for the mean first-passage time of random walks on a generalized koch network with a trap. *Chinese Physics B*, 21(3), 038901.

- Jolliffe, I. T. (1986). Principal components in regression analysis. In *Principal component analysis* (pp. 129–155). Springer.
- Kroese, D. P., Brereton, T., Taimre, T., & Botev, Z. I. (2014). Why the monte carlo method is so important today. *Wiley Interdisciplinary Reviews: Computational Statistics*, 6(6), 386–392.
- Lee, J., Lapira, E., Yang, S., & Kao, A. (2013). Predictive manufacturing system-trends of next-generation production systems. *IFAC Proceedings Volumes*, 46(7), 150–156.
- Manwell, J. F., McGowan, J. G., & Rogers, A. L. (2010). *Wind energy explained: theory, design and application*. John Wiley & Sons.
- Mei, Q., Gül, M., & Boay, M. (2019). Indirect health monitoring of bridges using mel-frequency cepstral coefficients and principal component analysis. *Mechanical Systems and Signal Processing*, 119, 523–546.
- Monitoring, S. C. (1994). *Vibration diagnostic guide*. Revision.
- Montgomery, D. C. (2017). *Design and analysis of experiments*. John Wiley & Sons.
- Murthy, K., & Kehr, K. (1989). Mean first-passage time of random walks on a random lattice. *Physical Review A*, 40(4), 2082.
- Nelson, W. (1972). Graphical analysis of accelerated life test data with the inverse power law model. *IEEE Transactions on Reliability*, 21(1), 2–11.
- Nelson, W. (1980). Accelerated life testing-step-stress models and data analyses. *IEEE transactions on reliability*, 29(2), 103–108.
- Omer, M., Margetts, L., Hadi Mosleh, M., Hewitt, S., & Parwaiz, M. (2019). Use of gaming technology to bring bridge inspection to the office. *Structure and Infrastructure Engineering*, 1–16.
- Paris, P., & Erdogan, F. (1963). A critical analysis of crack propagation laws.
- Pearson, K. (1901). Liii. on lines and planes of closest fit to systems of points in space. *The London, Edinburgh, and Dublin Philosophical Magazine and Journal of Science*, 2(11), 559–572.
- Phuc, D. V., Levrat, E., Voisin, A., & Benoit, I. (2012). Remaining useful life (rul) based maintenance decision making for deteriorating systems. *IFAC Proceedings Volumes*, 45(31), 66–72.
- Ploszajski, A. (2016, January). *Material of the month – silicon carbide*. Materials World magazine.

- Primožic, T. (2011). Estimating expected first passage times using multilevel monte carlo algorithm. *Master Thesis*.
- Qin, A., Zhang, Q., Hu, Q., Sun, G., He, J., & Lin, S. (2017). Remaining useful life prediction for rotating machinery based on optimal degradation indicator. *Shock and Vibration, 2017*.
- Rausand, M. (2014). *Reliability of safety-critical systems: Theory and applications*. Hoboken, NJ: Wiley.
- Rausand, M., & Høyland, A. (2004). *System reliability theory: Models, statistical methods, and applications* (2nd ed.). Hoboken, NJ: Wiley.
- Redner, S. (2001). *A guide to first-passage processes*. Cambridge University Press.
- Ross, S. M. (2014). *Introduction to probability models*. Academic press.
- Rossi, R. J. (2018). *Mathematical statistics: an introduction to likelihood based inference*. John Wiley & Sons.
- Saddik, A. E. (2018). Digital twins: The convergence of multimedia technologies. *IEEE MultiMedia, 25* (2): 87–92. doi:10.1109/MMUL.2018.023121167. ISSN 1070-986X.
- Saidi, L., Ali, J. B., Bechhoefer, E., & Benbouzid, M. (2017). Wind turbine high-speed shaft bearings health prognosis through a spectral kurtosis-derived indices and svr. *Applied Acoustics, 120*, 1–8.
- Sato, S., & Inoue, J. (1994). Inverse gaussian distribution and its application. *Electronics and Communications in Japan (Part III: Fundamental Electronic Science), 77*(1), 32–42.
- Saxena, A., Celaya, J., Saha, B., Saha, S., & Goebel, K. (2010). Metrics for offline evaluation of prognostic performance. *International Journal of Prognostics and health management, 1*(1), 4–23.
- Shepp, L. A. (1967). A first passage problem for the wiener process. *The Annals of Mathematical Statistics, 38*(6), 1912–1914.
- Tahmasebinia, F., Fogerty, D., Wu, L. O., Li, Z., Sepasgozar, S. M. E., Zhang, K., ... Marroquin, F. A. (2019). Numerical analysis of the creep and shrinkage experienced in the sydney opera house and the rise of digital twin as future monitoring technology. *Buildings, 9*(6), 137.
- Tao, F., Sui, F., Liu, A., Qi, Q., Zhang, M., Song, B., ... Nee, A. (2019). Digital twin-driven product design framework. *International Journal of Production Research, 57*(12), 3935–3953.

- Thomas, M. U. (1975). Some mean first-passage time approximations for the ornstein-uhlenbeck process. *Journal of Applied Probability*, 12(3), 600–604.
- Tian, J., Morillo, C., Azarian, M. H., & Pecht, M. (2015). Motor bearing fault detection using spectral kurtosis-based feature extraction coupled with k-nearest neighbor distance analysis. *IEEE Transactions on Industrial Electronics*, 63(3), 1793–1803.
- Tseng, S.-T., Tang, J., & Ku, I.-H. (2003). Determination of burn-in parameters and residual life for highly reliable products. *Naval Research Logistics (NRL)*, 50(1), 1–14.
- Urdapilleta, E. (2011). Survival probability and first-passage-time statistics of a wiener process driven by an exponential time-dependent drift. *Physical Review E*, 83(2), 021102.
- Vatn, J. (2018). Industry 4.0 and real-time synchronization of operation and maintenance. In *Safety and reliability-safe societies in a changing world-proceedings of the 28th international european safety and reliability conference, esrel 2018* (pp. 681–686).
- Vatn, J. (2019, September). *Tpk4161 - supply chain analytics*. (Equation 2.25)
- Vatn, J. (2020). Lecture memo for numerical integration of stochastic processes. *Course memo*, 5–8.
- Wang, G., Zhang, Y., Liu, C., Xie, Q., & Xu, Y. (2019). A new tool wear monitoring method based on multi-scale pca. *Journal of Intelligent Manufacturing*, 30(1), 113–122.
- Wang, Y., Ma, X., & Joyce, M. J. (2016). Reducing sensor complexity for monitoring wind turbine performance using principal component analysis. *Renewable energy*, 97, 444–456.
- Wiener, N. (1976). *Collected works, vol. 1, p. masani*. Cambridge (Mass.): MIT Press.
- Xu, Y., Sun, Y., Liu, X., & Zheng, Y. (2019). A digital-twin-assisted fault diagnosis using deep transfer learning. *IEEE Access*, 7, 19990–19999.
- Ye, Z.-S., & Xie, M. (2015). Stochastic modelling and analysis of degradation for highly reliable products. *Applied Stochastic Models in Business and Industry*, 31(1), 16–32.